

Article

Satellite-Based Meteorological and Agricultural Drought Monitoring for Agricultural Sustainability in Sri Lanka

Niranga Alahacoon^{1,2,*}, Mahesh Edirisinghe¹  and Manjula Ranagalage³ ¹ Department of Physics, University of Colombo, Colombo 00300, Sri Lanka; mahesh@phys.cmb.ac.lk² International Water Management Institute (IWMI), 127, Sunil Mawatha, Pelawatte, Colombo 10120, Sri Lanka³ Department of Environmental Management, Faculty of Social Sciences and Humanities, Rajarata University of Sri Lanka, Mihintale 50300, Sri Lanka; manjularanagalage@ssh.rjt.ac.lk

* Correspondence: n.alahacoon@cgiar.org

Abstract: For Sri Lanka, as an agricultural country, a methodical drought monitoring mechanism, including spatial and temporal variations, may significantly contribute to its agricultural sustainability. Investigating long-term meteorological and agricultural drought occurrences in Sri Lanka and assessing drought hazard at the district level are the main objectives of the study. Standardized Precipitation Index (SPI), Rainfall Anomaly Index (RAI), and Vegetation Health Index (VHI) were used as drought indicators to investigate the spatial and temporal distribution of agriculture and meteorological droughts. Climate Hazards Group Infrared Precipitation with Stations (CHIRPS) data from 1989 to 2019 was used to calculate SPI and RAI. MOD13A1 and MOD11A2 data from Moderate Resolution Imaging Spectroradiometer (MODIS) from 2001 to 2019, were used to generate the Vegetation Condition Index (VCI) and Temperature Condition Index (TCI). Agricultural drought monitoring was done using VHI and generated using the spatial integration of VCI and TCI. Thus, various spatial data analysis techniques were extensively employed for vector and raster data integration and analysis. A methodology has been developed for the drought declaration of the country using the VHI-derived drought area percentage. Accordingly, for a particular year, if the country-wide annual extreme and severe drought area percentage based on VHI drought classes is $\geq 30\%$, it can be declared as a drought year. Moreover, administrative districts of Sri Lanka were classified into four hazard classes, No drought, Low drought, Moderate drought, and High drought, using the natural-beak classification scheme for both agricultural and meteorological droughts. The findings of this study can be used effectively by the relevant decision-makers for drought risk management (DRM), resilience, sustainable agriculture, and policymaking.

Keywords: drought; agricultural drought; meteorological drought; drought hazards; remote sensing; MODIS; spatial analysis; CHIRPS data; rainfall; VHI



Citation: Alahacoon, N.; Edirisinghe, M.; Ranagalage, M. Satellite-Based Meteorological and Agricultural Drought Monitoring for Agricultural Sustainability in Sri Lanka. *Sustainability* **2021**, *13*, 3427. <https://doi.org/10.3390/su13063427>

Academic Editor: Amir Mosavi

Received: 18 February 2021

Accepted: 15 March 2021

Published: 19 March 2021

Publisher's Note: MDPI stays neutral with regard to jurisdictional claims in published maps and institutional affiliations.



Copyright: © 2021 by the authors. Licensee MDPI, Basel, Switzerland. This article is an open access article distributed under the terms and conditions of the Creative Commons Attribution (CC BY) license (<https://creativecommons.org/licenses/by/4.0/>).

1. Introduction

Drought is a natural phenomenon that occurs recurrently, causing widespread depletion of natural or manmade water resources over a large geographical area during a considerable period [1]. It is natural for drought regions to experience extreme water shortages due to delays in rainfall, insufficient rainfall, and high surface water evaporation caused by overheating [2]. Therefore, drought has a significant adverse effect on agriculture, socioeconomic activities, and the natural ecosystem [3]. Drought is relatively more severe than any other hydro-meteorological hazard, affecting more people and their crops to a broader geographical extent [4]. In the last two decades, the economic loss to the world due to drought has been reported in the thousands of billions, and the number of people affected by the drought has exceeded one billion [5]. As a result of climate change, global warming is expected to lead to more severe droughts, both globally and regionally, with increased drought risk [6–10].

Although Sri Lanka is a tropical country, it has been hit by many extreme to severe droughts over the past few decades, and their adverse effects have severely affected the country's economy [11,12]. According to various studies and reports, there were 14 drought events that had been recorded during the period from 1980 to 2019 in Sri Lanka [13–15]. Moreover, about 52% of crop damage from 1974 to 2013 was caused by drought, alone [12]. The droughts recorded during 2001, 2002, 2016, and 2017 were of great concern to Sri Lanka [12,15]. A continuous drought reported in 2001 and 2002 severely affected the country's hydropower generation and agriculture sector, reducing its GDP by about 1% [12]. Therefore, identifying drought-prone areas through the study of the occurrence and spatial distribution of historical droughts in Sri Lanka would be of utmost importance in selecting drought mitigation measures to reduce the future drought risk.

However, a better understanding of drought is needed to determine the spatial-temporal occurrence of it, because the drought is a very complex process. It is also challenging to determine the exact beginning and end of a drought, and, often, the effects of drought can last even longer after a severe drought [16]. Droughts are generally classified into four major types: meteorological, agricultural, hydrological, and socioeconomic [17]. These four types of droughts are interlinked and come one after the other; for example, agricultural droughts occur sometime after the meteorological drought. Meteorological drought is defined as a prolonged dry weather period that dominates an area due to a long delay or lack of rainfall events [18]. Agricultural droughts occur when crops are damaged, and this drought coincides more closely with the meteorological drought, but the crop stage determines the time interval between the two droughts [19]. Hydrological droughts usually occur several months after the onset of meteorological drought, and the main reason for this is the prolonged lack of rainfall, which significantly reduces the flow of rivers, reservoirs, and groundwater levels. Although meteorological drought recovery is short, hydrological drought recovery takes a long time [20].

Rainfall is the major contributing factor to drought, and the effects of drought are reflected in declining water levels in reservoirs, declining soil moisture, reduced river flow, and declining groundwater levels [21]. Thus, many scientists have developed various methods and indices for studying and monitoring droughts for more than half a century, using both catalyst (precipitation, temperature, soil moisture, evapotranspiration, humidity) and response (vegetation health and reservoir and groundwater levels) parameters [22–28]. The uniqueness of drought indices is that they can illustrate the severity and magnitude of a drought event [29]. Usually, it does not show a reliable correlation among different drought indices, and it is common for some drought indices to indicate drought in one area but not for others [30].

Although a large number of drought indices have been developed for meteorological drought monitoring, the major indices are the Palmer Drought Intensity Index (PDSI), the Standardized Precipitation Index (SPI), Rainfall Anomaly Index (RAI), and the Standardized Precipitation Evapotranspiration Index (SPEI) [22,31]. Compared to other meteorological drought indicators, SPI and RAI have been used in many studies, as they have a better ability to characterize the dryness and wetness of the area [32–40]. The SPI and RAI indices can be introduced as straightforward and flexible indices to monitor drought at different timeframes with a -3 to $+3$ index scale. Furthermore, various researchers have shown that an increase in the number of non-rainy days mainly contributes to drought occurrence [41], and some studies have shown that climate change has increased the number of dry days in some areas and increased the likelihood of heavy rains by keeping the total annual rainfall unchanged.

Traditionally, drought monitoring relied on hydrological meteorological measurements obtained from local gauge stations [42,43]. Even though the rainfall stations' data are more accurate, they are less suitable for continuous drought monitoring, due to sparse observation nets, scale mismatches, and the fact that they only apply to a small surrounding area [44]. Therefore, satellite remote sensing can be used as a more viable option to minimize those disadvantages of location-specific drought monitoring [45,46]. It provides

a sound approach to measure the variability of drought monitoring parameters with high spatial and temporal resolution through near-real-time observations [46]. For example, Climate Hazards Group Infrared Precipitation with Stations (CHIRPS) data are decent substitutes for station-based rainfall data, as these data have been estimated via satellites and have increased accuracy through the station data integration [41,47]. Furthermore, the validity of CHIRPS data has been confirmed by several studies using gauge precipitation data for (OR within) many regions of the world and used to develop a large number of studies on drought [48,49].

Agriculture drought indices generated using satellite data in drought monitoring and assessment as the best auxiliary for the station data are very popular all over the world, due to their unique features, such as low cost, synoptic view, data recurrence, and reliability [50]. The use of Normalized Difference Vegetation Index (NDVI), Temperature Condition Index (TCI), and Vegetation Condition Index (VCI) for agricultural drought identification and monitoring is globally recognized [51–54]. Those indicators' uniqueness is their autonomy from different environmental conditions [55,56].

Since Sri Lanka is an agricultural country and is prone to frequent droughts, systematic drought monitoring can significantly contribute to the sustainable development of agriculture. Moreover, over the past few decades, many studies have been conducted to monitor the drought in Sri Lanka, and most of these studies are SPI-based drought analyses based on location-specific rainfall data [14,57–59]. However, most of those studies have not paid much attention to map the spatial–temporal patterns and drought hazards. The spatial distribution of drought is not adequately represented, as only location-specific data have been used for those studies. Therefore, it is timely and important to perform a comprehensive drought analysis representing the spatial distribution of drought in agricultural planning, disaster management, and drought mitigation [14,59]. Henceforth, this study specifically focuses on investigating the use of satellite-based drought monitoring for Sri Lanka's agricultural sustainability.

This study was intended to monitor the pattern of long-term rainfall over months, seasons, and years and to assess the extent to which changes in daily rainfall have affected drought. The main objective of this study was to monitor long-term meteorological and agricultural drought patterns in Sri Lanka. CHIRPS-derived Rainfall Anomaly Index (RAI) and the Standardized Precipitation Index (SPI) were used to monitor the meteorological drought, while Moderate Resolution Imaging Spectroradiometer (MODIS)-based Vegetation Condition Index (VCI), Temperature Condition Index (TCI), and Vegetation Health Index (VHI) were used for agricultural drought monitoring. Furthermore, the study has been extended to assess district-wide drought hazards based on the long-term occurrence of meteorological and agricultural droughts in Sri Lanka. Another objective of the study is to introduce a novel drought declaration mechanism through a quantitative approach. An attempt has also been made to observe the impact on the country's economy in conjunction with the respective years in which severe droughts in Sri Lanka have occurred. The results of the study could be effectively used for disaster risk management (DRM), disaster resilience, and achieving sustainable agriculture.

2. Study Area, Spatial Data, and Methodology

2.1. Study Area

Sri Lanka is an agricultural island in nature with a tropical climate, located in the southwestern part of the Indian Ocean and below India at latitudes 5–10° N and longitudes 79–82° E (Figure 1). Sri Lanka covers 65,610 km² and has a coastline of 1340 km, with a population of 22 million. Moreover, Sri Lanka is divided into four climatic zone, wet zone (>2500 mm), dry zone (1800–2500 mm), intermediate zone (1200–1800 mm), and semiarid zone (<1200 mm), categorized using the average of long-term annual rainfall [60]. Moreover, there are four rainfall seasons (monsoon seasons) identified in Sri Lanka that directly affect the annual rainfall, namely northeast monsoon (NEM—December to February), first inter-monsoon (FIM—March to April), southwest monsoon (SWM—May to September), and the

second inter-monsoon (SIM—October to November) [61]. According to these four tropical rainy seasons, in Sri Lanka, two cultivation seasons, known as “Yala” and “Maha,” can be identified. Yala season is from April to September, and Maha season is from October to March next year [62]. Sri Lanka is one of the most affected countries, in terms of the percentage of the population affected by various natural disasters, and is ranked second among the affected countries in the Global Climate Risk Index published in 2019 [63]. Furthermore, drought is one of the most severe natural disasters affecting agriculture in Sri Lanka and has affected various parts of the country in different intensities.

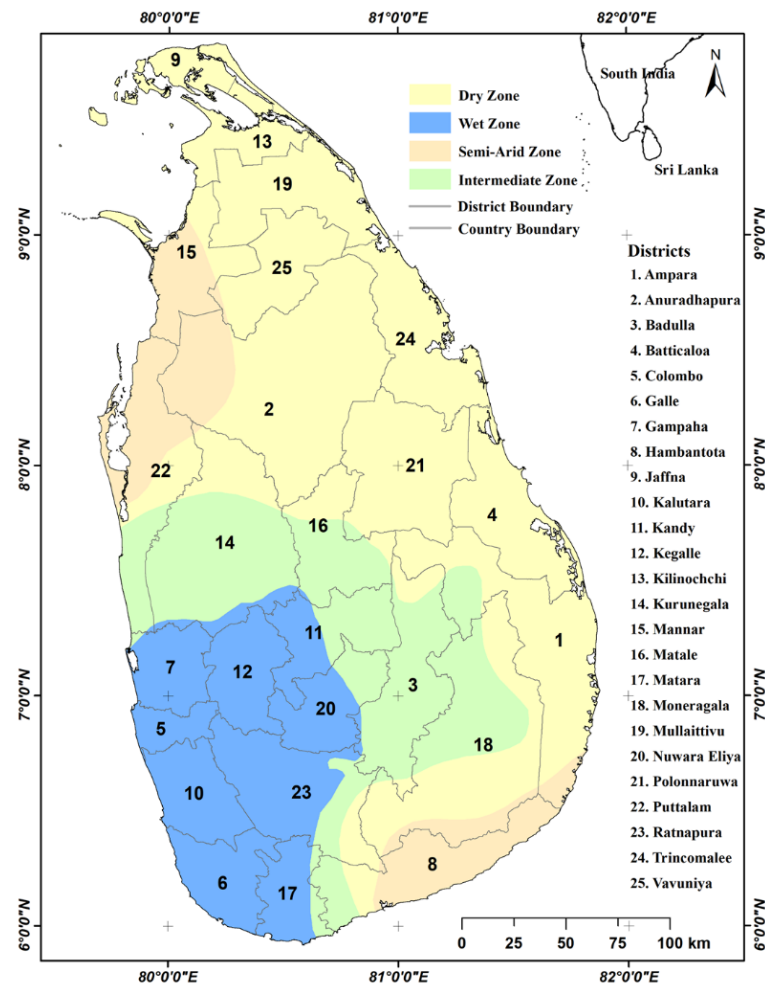


Figure 1. District and climate zone boundaries of Sri Lanka.

Moreover, in order to understand how the variability of rainfall reported at the district level contributes to different climatic zones, it is important to identify the percentage of areas represented by different districts for the respective climatic zones. The district area percentages for the four climatic zones are represented in Table A1.

2.2. Spatial Data

In this study, Climate Hazards Group Infrared Precipitation with Stations (CHIRPS) daily rainfall [64] and terra-MODIS (Terra Moderate Resolution Imaging Spectroradiometer) monthly NDVI and Land Surface Temperature (LST) data were used to calculate the meteorological and agricultural drought in Sri Lanka. CHIRPS rainfall products are available as gridded data at daily time intervals, and they were downloaded from the Climate Hazard Center covering 1989 to 2019. The CHIRPS data products provided with a spatial resolution of 5 km that have been developed by integrating satellite estimated rainfall with ground-measured rainfall data. However, agricultural drought monitoring cannot be done

using CHIRPS data, alone, as it does not capture vegetation responses. Therefore, crop responses to drought are best captured by satellite data and are widely used for agricultural drought monitoring.

The MODIS product, also known as MOD11A2, with a spatial resolution of one kilometer, is available to represent the Land Surface Temperature (LST) every eight days [65]. That data is available for free download from the National Aeronautics and Space Administration (NASA) Earth Data portal at 8-day intervals. The MOD11A2 product consists of both day and night temperature as two separate layers. The MOD13A3 product is also available at the NASA-Earth Data portal monthly time interval with 1 km spatial resolution. NDVI, Enhanced Vegetation Index (EVI), and quality control bands (QC-bands) are available in this data product [66]. The NDVI and LST were used to generate the VCI and TCI from 2001 to 2019, while CHIRPS data were used to generate RAI and SPI from 1989 to 2019.

2.3. Methodology

Figure 2 shows a detailed overview of the flow representation of the methodology used for the study. This flow chart provides the overall picture of the data usage and statistical parameters, as well as equations that were used for drought index computations in the study. Henceforth, the calculation of the number of dry days and wet days, Standardized Precipitation Index (SPI), Rainfall Anomaly Index (RAI), Vegetation Condition Index (VCI), Temperature Condition Index (TCI), Vegetation Health Index (VHI), and drought hazard are explained in detail.

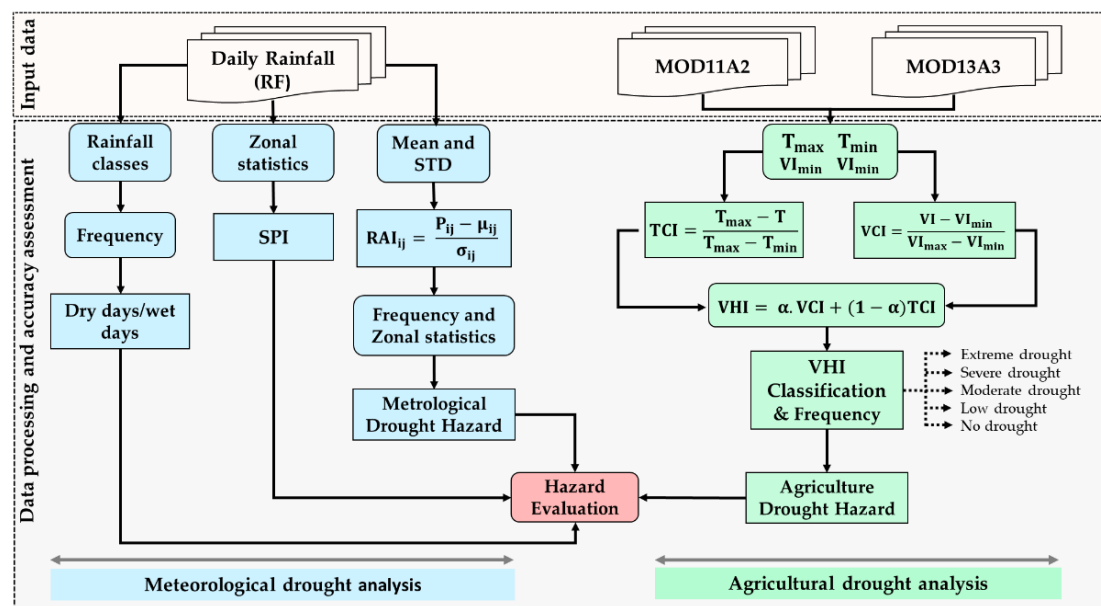


Figure 2. Methodology flowchart for the study. SD stands for Stand deviation, T for temperature, P for Rainfall, and VI for Vegetation index.

2.3.1. Number of Wet and Dry Days Calculation

In order to study the occurrence of drought and its persistence due to changes in rainfall patterns, different rainfall classes are used as representations in Table 1. Daily CHIRPS rainfall raster data were used to classify according to those rainfall classes. This classification procedure was applied to 11,315 raster layers, and each covers daily rainfall of 31 years, from 1989 to 2019, to generate binary raster information. Then the binary layers were produced for Dry, Light, Moderate, Rather Heavy, Heavy and Very Heavy rain classes. Then, the number of average days of occurrence in different rainfall classes for the four rainy seasons (SWM, NEM, FIM, and SIM) was calculated separately.

Table 1. Classification of daily rainfall [67].

Class	Rainfall (R) in a Day (mm)
Dry	<2.0
Light	2.0 > R < 10.0
Moderate	10.0 > R < 33.5
Rather heavy	33.5 > R < 64.4
Heavy	64.4 > R < 124.4
Very heavy	>124.4

2.3.2. Calculation of Rainfall Anomaly Index (RAI)

The Rainfall Anomaly Index (RAI) can be introduced as an essential and useful indicator in studying and analyzing meteorological droughts [68]. This indicator appears to be a simple index that is easy to calculate, compared to other drought indicators. This index can also be calculated using different time dimensions, such as monthly, seasonal, or annual. In this study, the annual, seasonal, and monthly accumulated rainfall of Sri Lanka for 31 years from, 1989 to 2019, were calculated using CHIRPS daily data. After that, the rainfall anomaly index for the above time dimensions was calculated using Equation (1). In the RAI calculation, a particular rainfall is a negative value if it is less than a long-term average and a positive if it is more. Negative values always represent drought, and the magnitude of that value determines the magnitude of the drought.

$$RAI_{ij} = \frac{P_{ij} - \mu_{ij}}{\sigma_{ij}} \quad (1)$$

where, P is rainfall, μ and σ are the long-term mean and standard deviation of *i*th timeframe at *j*th timescale.

2.3.3. Standardized Precipitation Index (SPI)

The SPI is designed to determine meteorological drought at multiple time intervals. Long-term rainfall data are required to calculate the SPI, and those data are then subjected to a probability distribution and then to a normal distribution, keeping the median SPI at zero for a desired location or period [69]. SPI values vary from -3 to $+3$, and, according to the calculation, the rain that is higher than the median rainfall is given as a positive SPI, while a negative value represents less than the median [26]. Gamma distribution is defined by its frequency or probability function as in Equation (2).

$$g(x) = \frac{x^{\alpha-1} \cdot e^{-\frac{x}{\beta}}}{\beta^{\alpha} \cdot \Gamma(\alpha)} \text{ for } x > 0 \quad (2)$$

where, " α " and " β " are the parameters of shape and scale, x is the amount of precipitation, and $\Gamma(a)$ is the gamma distribution function. Equations (3) and (4) are used to calculate the α and β parameters.

$$\alpha = \frac{1}{4A} \left[1 + \sqrt{1 + \frac{4A}{3}} \right] \quad (3)$$

$$\beta = \frac{x}{a} \text{ where } A = (x) - \frac{\sum \ln(x)}{n} \quad (4)$$

where, n is the number of rainfall records.

The gamma function is not defined for $x = 0$, and the cumulative probability is calculated using Equation (5), since zero precipitation is the most common occurrence in terms of precipitation.

$$H(x) = q + (1 - q)G(x) \quad (5)$$

The probability of zero precipitation is given as q , and $G(x)$ is the gamma function's cumulative probability. The cumulative probability $H(x)$ is then converted to the standard

normal distribution (z) using the mean of zeros and the variance of one, and the result is SPI. Based on the SPI methodology described above, SPI was generated using World Meteorological Organization (WMO)–SPI software covering all districts and climatic zones of Sri Lanka from 1989 to 2019. Furthermore, the SPI was calculated for different time sequences as 1, 3, 6, 9, 12, and 24 months, so that the long-term and short-term variability of the drought could be identified. The SPI value classification, according to the drought classes provided in Table 2 and SPI values of 1–3 months, can be used to identify short-term droughts, 6–9 months of monsoon droughts, and 12–24 months of long-term and interannual droughts.

Table 2. Standardized Precipitation Index (SPI) drought classes based on its values and probability distribution [26].

Class No	Drought Class	SPI Value Range	% of Probability
1	Extreme drought	$SPI \leq -2$	2.3
2	Severe drought	$-2 < SPI \leq -1.5$	4.4
3	Moderate drought	$-1.5 < SPI \leq -1$	9.2
4	Normal	$-1 < SPI \leq 1$	68.2
5	Moderately wet	$1 < SPI \leq 1.5$	9.2
6	Severe wet	$1.5 < SPI \leq 2$	4.4
7	Extreme wet	$SPI > 2$	2.3

2.3.4. Vegetation Condition Index (VCI)

Although NDVI has successfully identified well-grown and stressed crops, interpretation problems often arise, due to changes in vegetation levels and environmental resources, such as climate, soil, and vegetation in a given area. For instance, NDVI can be strongly differentiated between a single crop for a resource-rich area and a nonabundant area. Therefore, it is possible to identify the two components in NDVI as ecological and climatic, and it is difficult to observe differences between the two components for the intense or high vegetation zone. The NDVI value, alone, makes it challenging to identify the climatic component of crops, and researchers designed the VCI index to easily identify the weather impact on crops [25]. The Vegetation Condition Index (VCI) can be calculated using Equation (6).

$$VCI = \frac{NDVI - NDVI_{\min}}{NDVI_{\max} - NDVI_{\min}} \quad (6)$$

where, the maximum value of the VCI index is in the range of 100, and the minimum is 0, which is close to 100 in suitable crop environments and close to 0 in bad crop conditions.

2.3.5. Temperature Condition Index (TCI)

The Temperature Condition Index (TCI) is calculated using long-term temperature data, widely used by various researchers to determine vegetation's stress due to temperature variation [51]. The calculation of TCI values is done inversely to the VCI with Equation (7), considering that the increase in temperature will affect vegetation growth. In such a calculation, both the TCI and VCI indices' values are in the same scale and dimensions, and the increase in their values indicates a favorable situation for the crop.

$$TCI = \frac{T_{\max} - T}{T_{\max} - T_{\min}} \quad (7)$$

Temperature conditions at any given time are calculated using the maximum and minimum temperatures of the considered period. Low values of TCI indicate adverse conditions for the crop, and high values indicate favorable conditions. In the case of crops, the temperature is most affected in the early stages of the crop, but a gradual increase in temperature indicates drought.

2.3.6. Vegetation Health Index (VHI)

For nearly three decades, many researchers have used the VHI index to identify agricultural droughts, their duration, and the impact of different geographical regions globally [52,70]. Combining VCI and TCI with the following Equation (8), the VHI indicator is designed to determine crop health status.

$$\text{VHI} = \alpha \cdot \text{VCI} + (1 - \alpha) \text{TCI} \quad (8)$$

The α is the contributing factor for both VCI and TCI. In most studies, the VHI drought index is calculated by keeping the value of α at 0.5, and the VHI value is scattered in the range of 0 to 100. Low VHI values are indicative of drought, while high values indicate vigorous vegetation.

2.3.7. Drought Frequency and Hazard

RAI and VHI indexes are used to calculate the frequency of meteorological and agricultural drought hazards, respectively. Drought classes of VHI, called extreme, severe, and moderate, were used to calculate drought frequencies from 2001 to 2019. For meteorological drought hazard mapping, annual RAI data from 1989 to 2019 were used, and RAI values -1.5 were used as a threshold for annual drought binary extraction. Drought layers calculated for each month were classified according to the drought classes in each index, and then binary layers were produced to represent only the drought classes. The frequency of droughts per year was calculated using the calculated monthly binary estimates, and the average, minor, moderate, and severe levels of drought were classified according to the frequency of the annual drought using the natural-breaks method. Annual binary layers were then generated using only the moderate and severe drought classes, and these maps were accumulated with the sum for all years to calculate the frequency of long-term drought at the district level or each pixel level. Finally, the above-processed layers were subject to spatial normalization (0–100) using maximum and minimum frequencies to identify drought hazards at the pixel level, and the no drought, low, moderate, and high drought classes were determined through natural-breaks classification. Equation (9) applies to the calculation of drought frequency.

$$F_j = \left(\frac{n_j}{N} \right) * 100 \quad (9)$$

Drought frequency is F_j , and j is the drought class. n_j indicates how many times the drought level j occurred through the relevant layers. N is the total number of drought layers used for the study.

3. Results

This study's initial face provides the context for the analysis of long-term annual average rainfall covering the whole of Sri Lanka monthly, during each monsoon season, and annually for a period of 31 years, from 1989 to 2019.

3.1. Long-Term Rainfall Average at District and Climate Zones

Table A2 shows how the 31 years average rainfall changes at the climatic zone and district level. The crop's maximum growth and maturity during the Yala season are in June and July, but Table A2 clearly shows that the average rainfall received by all the districts in the dry zone during those two months is less than 40 mm. This means that crop cultivation in the dry zone should be carried out with proper water management in the Yala season. Otherwise, the crop is more vulnerable to drought. SIM receives the highest rainfall in all districts, but the semiarid zone districts receive the lowest rainfall in all seasons.

The wet zone districts receive significant rainfall during all monsoon seasons, and even the dry zone receives comparably high rainfall than the SWM in FIM. Compared to the study conducted using gauge rainfall data from 1976 to 2006 [71], this study shows

that districts in the intermediate zone of Kurunegala, Matale, and Badulla receive higher rainfall during the NEM and SIM seasons. On the other hand, it appears that the average rainfall for all the districts in the wet zone during the last 31 years has exceeded 100 mm in all the months, i.e., this region is wet, and the chances of drought are much less. However, considering the variability of annual average rainfall in the climatic zones, the values of the wet, dry, and intermediate zones are consistent with the rainfall classification of the climatic zones. However, the semiarid zone's rainfall appears to be increasing 65 mm than the maximum average (1200 mm). This shows that the semiarid zone has moved slowly toward the dry zone for the last 31 years.

3.2. Wet Days and Dry Days in Monsoon Seasons

This section looks at how the number of rainy days for the four monsoon seasons in the country's wet, dry, intermediate, and semiarid climate zones over the past 31 years coincided with the drought. Figures 3 and 4 show how the number of rainy days recorded in the aforementioned climate zones varies for the different rainfall classes (Table 1). Figures 3 and 4 are arranged according to the southwest monsoon (SWM), northeast monsoon (NEM), first inter-monsoon (FIM), and second inter-monsoon (SIM), also known as the monsoon season in the country, and four graphs for four seasons are used to represent one climate zone.

These graphs can be used to understand how different rainfall classes and their number of events affect drought and distribution. In the wet zone, under all monsoon conditions, the Moderate rainfall class appears to be higher than that of the Light, and a significant increase in the number of days occurring in both classes can be observed. SWM has the highest incidence of Very Heavy and Heavy class and FIM and NEM have the lowest incidence. Another indication is that, during the drought period, the three classes of Light, Moderate, and Rather Heavy saw the number of days of rainfall decrease significantly.

The dry zone usually experiences more drought, while NEM and SIM receive the most rainfall for all classes. Yala season crops are controlled mainly by rainfall in both SWM and FIM seasons, but the study of SWM and FIM charts in the dry zone shows that the dry zone receives less rainfall in both seasons for all the rainfall classes. In both the SEM and FIM monsoons, the Light class is predominant, and the number of days is 15–35 and 5–20, respectively. Light, Moderate, and Rather Heavy rainfall classes during drought are also observed to be 20% to 60% lower than the average. Another important factor identified in this region is that the occurrence of drought in both the major crop seasons of Yala and Maha and the considerable reduction in the number of days of rainfall classes in Light, Moderate, and Rather Heavy coincide with each other. All other monsoon seasons except SIM show no significant increase in rainfall in this region.

In terms of the intermediate zone, its monsoon behavior is more or less similar to that of the dry zone, but SWM was receiving more days of rain than the dry zone. Light rainfall days in SWM and SIM in this region show a significant increase, but not all other classes. The pattern of precipitation days in the semiarid zone is similar to that of the dry zone but is characterized by higher values of the Light and Moderate classes in the dry and intermediate zones than in the SWM and FIM. However, Rather Heavy, Heavy, and Very Heavy show lower values for all other regions and all monsoons.

The number of heavy rainfall events varies from 1 to 5 for all climatic zones and rainy seasons. The peculiarity is that Very Heavy events in the dry zone in SWM are sporadic (only two cases), but a slight increase in such cases in the NEM can be detected in the wet zone. Heavy behaves similarly to Very Heavy, and about 90% of Heavy cases in SWM occur in the wet zone, while NEM is more prevalent in the dry zone, although Heavy events are scattered throughout Sri Lanka.

However, the main finding of the study of variability in small rainfall events (Light and Moderate) for all the seasons is that, in the years of drought, the number of rainy days of those two classes is 25–30% less than the average. However, the implication is that the lower number of rainy days in Light and Moderate classes is much more likely

to contribute to drought. In other words, the persistence of drought depends on how the wet and dry days are maintained during the monsoon season. Thus, the most important observation reflected in the representation of the variability of Light and Moderate rainfall occurrence over time is that those rainfall events caused by SWM in the dry zone are less than ten days in total, even in the non-drought years.

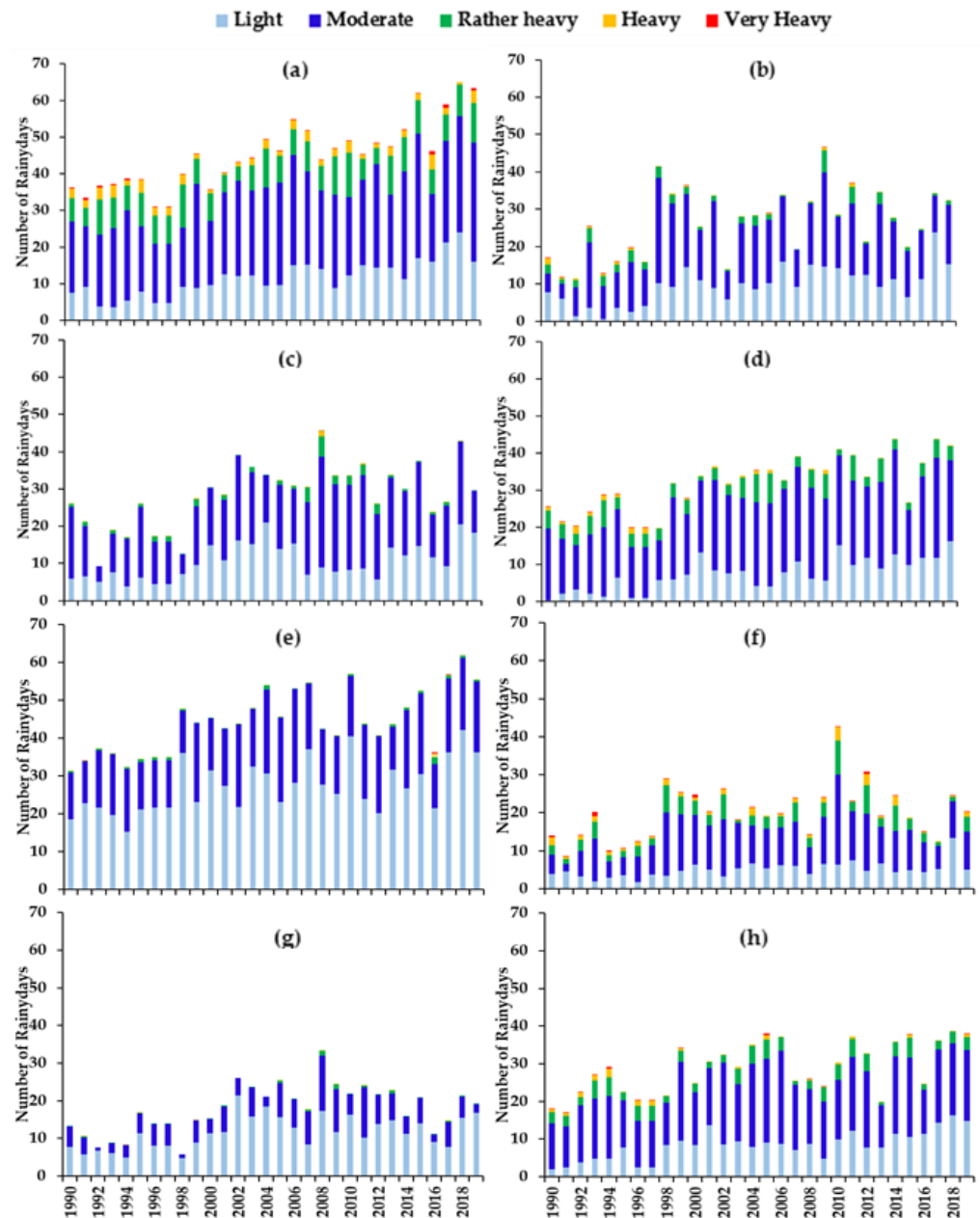


Figure 3. Mean number of rainy days exceeding the reported daily rainfall threshold level; bars and lines represent the number of rainy days in the classes defined in Table 1. The average number of rainy days in the wet zone (a–d) during southwest monsoon (SWM), northeast monsoon (NEM), first inter-monsoon (FIM), and second inter-monsoon (SIM), respectively, and (e–h) dry zone during SWM, NEM, FIM, and SIM, respectively.

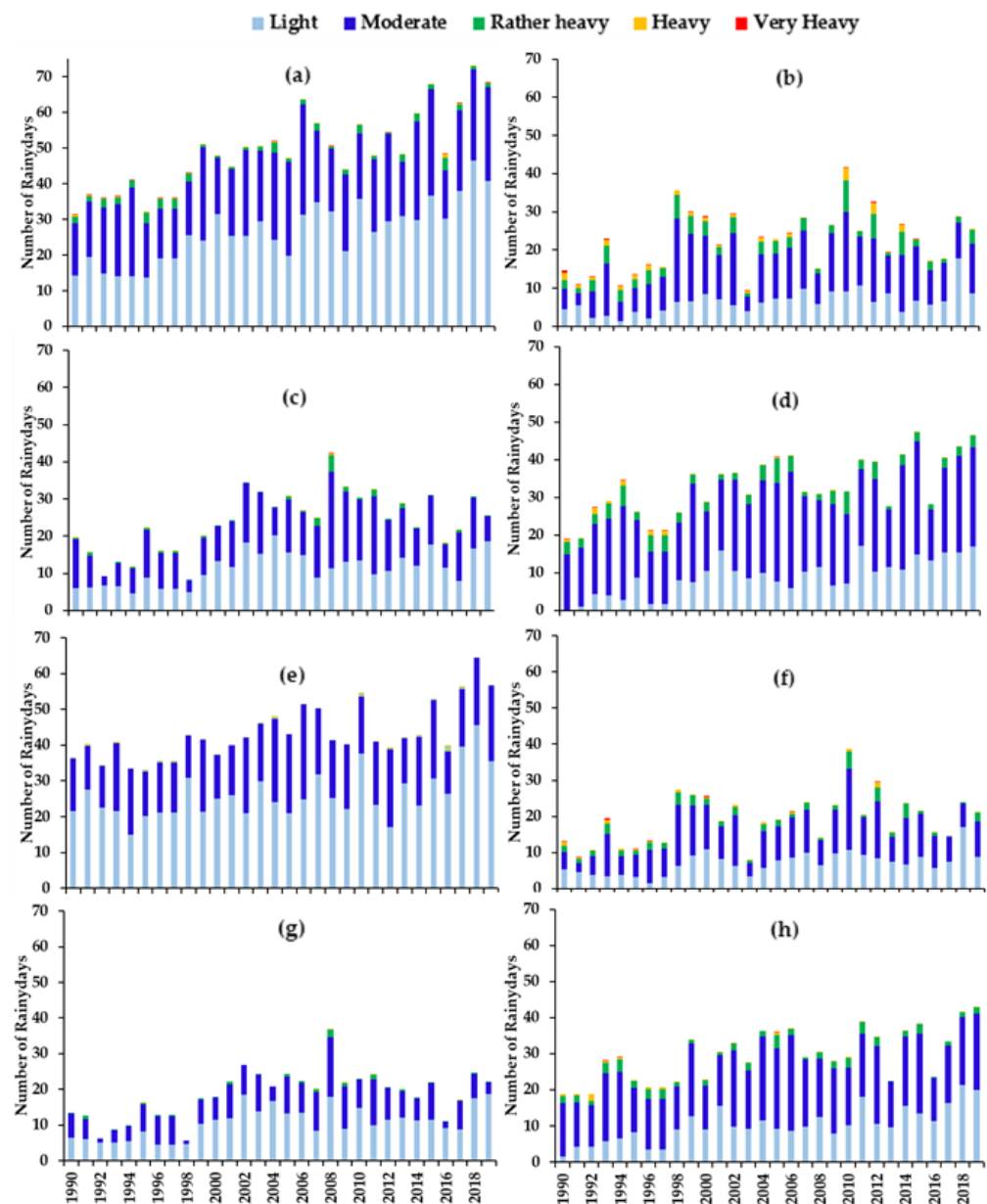


Figure 4. Mean number of rainy days exceeding the reported daily rainfall threshold level; bars and lines represent the number of rainy days in the classes, defined in Table 1. The average number of rainy days in the intermediate zone (a–d) during SWM, NEM, FIM, and SIM, respectively, and (e–h) semiarid zone during SWM, NEM, FIM, and SIM, respectively.

This means that the incidence of all types of rainfall during the “Yala” season is generally less in the dry zone. Overall, it appears that the reduction in the number of days of 2–10 and 10–30 mm of rainfall is closely related to the occurrence of drought. It is clear from these observations that the Light, Moderate, and Rather Heavy rain classes have the most significant impact on drought. Thus, the conclusion that can be made from all these observations is that a better understanding of drought can be obtained by studying the occurrence of Light, Moderate, and Rather Heavy rainy days.

Changes in Dry Days in Yala and Maha Crop Season

Figure 5 shows the variation of dry days in the wet, dry, intermediate, and semiarid zones during the Yala and Maha cropping seasons from 1989 to 2019. The most important thing that emerges here is the tendency for an apparent decrease in the number of non-rainy days from 1990 to 2019 for all the climatic zones.

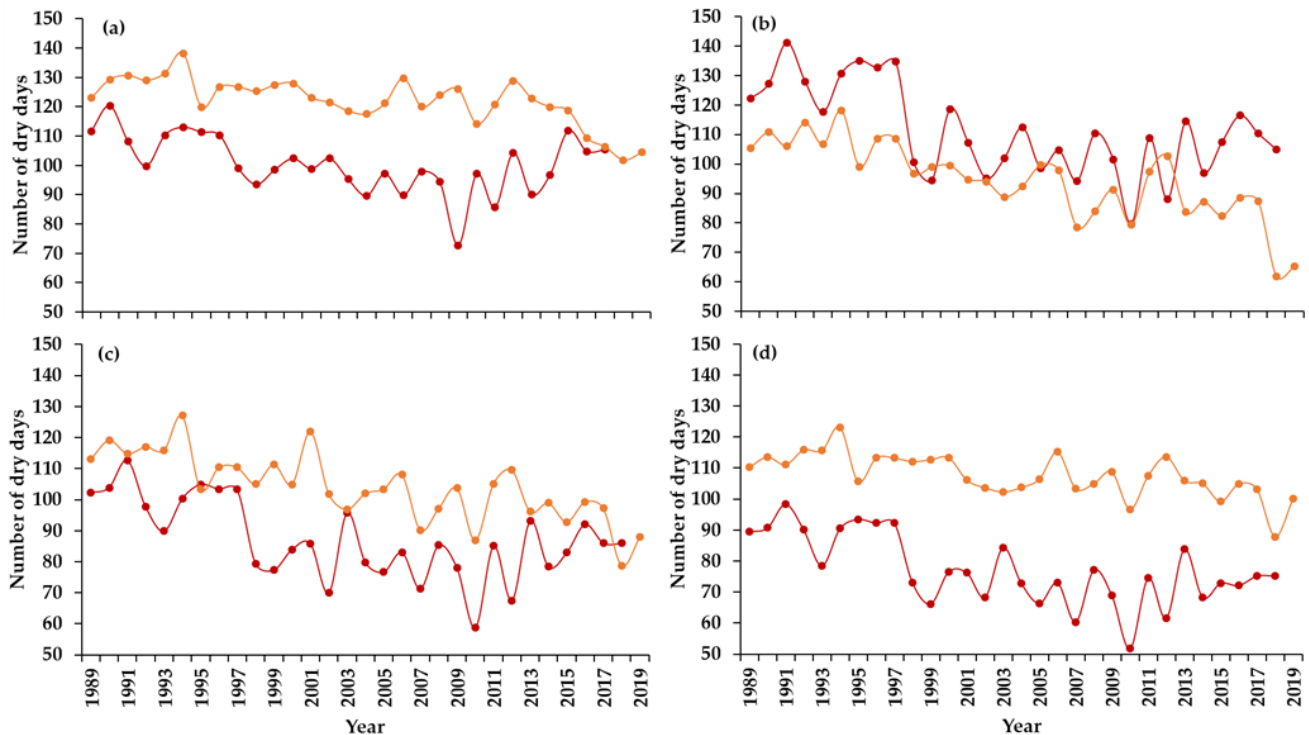


Figure 5. Variation of the number of dry days in the wet (a), dry (b), intermediate (c), and semiarid (d) zones over both Yala and Maha cropping seasons. (Total number of days for Yala season, 182, and Maha, 183).

This shows that the dry weather in Sri Lanka is gradually decreasing. However, further scrutiny of these graphs shows a strong correlation between the drought occurrences and the increase in non-rainy days, and the dry days in drought years show a decrease of 20–40 days, compared to the average dry days in the year.

3.3. Rainfall Anomaly (Annual and Monthly)

Preliminary drought studies can be carried out using the Rainfall Anomalies Index (RAI), a simple and essential indicator that can be effectively used in meteorological drought monitoring. Furthermore, using this RAI, rainfall variability can be calculated on different time scales, such as monthly, seasonally, or annually. Figure 6 shows the Rainfall Anomalies Index's variation generated using the annual and seasonal average rainfall of Sri Lanka from 1989 to 2019. Negative anomalies show dry years, and positive anomalies represent the wet year, and the length of the bar determines the intensity of drought or wetness on that chart. This analysis is a fair reflection of the droughts reported in Sri Lanka and their severity.

There was a severe drought in the 2016 Maha season, and, similarly, droughts were detected in 2017 and 2018 with low intensity. However, it is possible to identify whether or not there was a drought in any given year, but it is impossible to identify seasonal changes only with the annual RAI. The best solution to this is to analyze the RAI separately for Yala and Maha's two seasons. According to the Disaster Management Center, although the 2013 Yala season was a bumper crop season, the 2013–2014 Maha season was a drought season, as shown in Figure 6. The RAI analysis season drought shows more drought in the Yala season than in the Maha season from 1990 to 2019. However, after 2012, there is an

increasing drought in the Maha season, but no single prominent meteorological drought occurred during the Yala season.

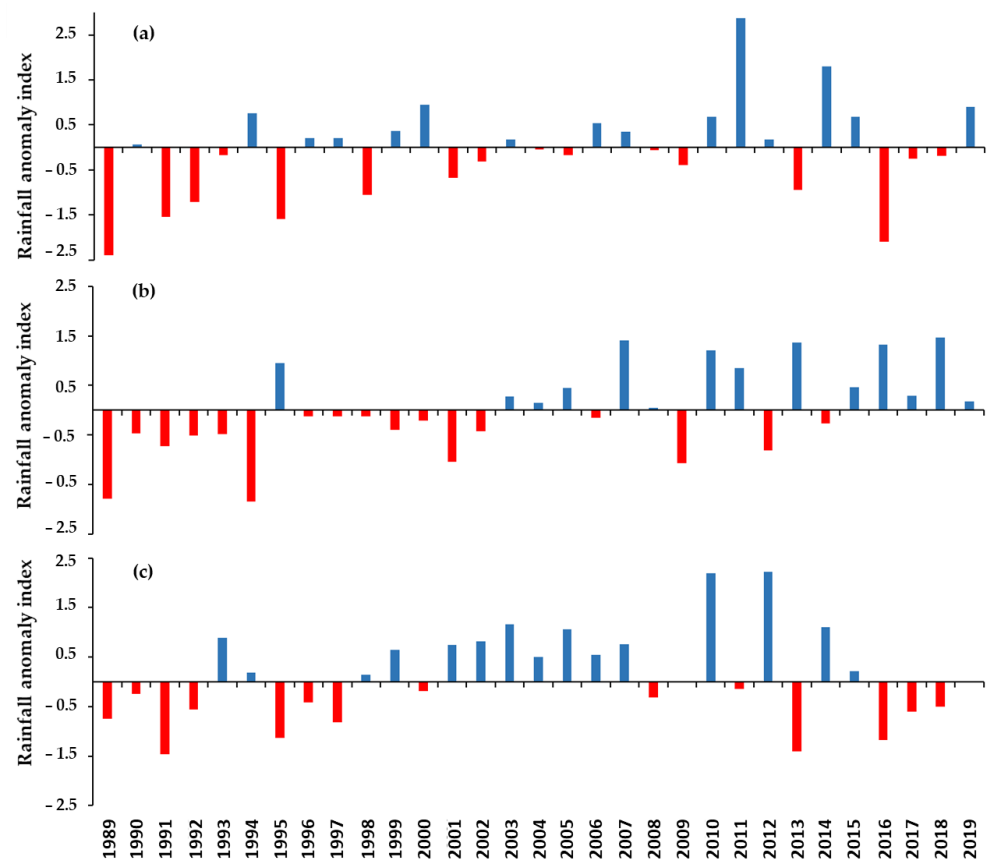


Figure 6. (a) Annual, (b) Yala, and (c) Maha season rainfall anomaly index from 1989 to 2019 in Sri Lanka.

However, the pixel-based RAI index, calculated at the monthly time frame, is more suitable for studying the spatial–temporal variability of drought during the Yala and Maha seasons. Figure 7 shows the spatial distribution of RAI values in Sri Lanka during both the Yala and Maha seasons for drought and non-drought years. It shows that the variations in the drought in the 2012 Yala and 2016–2017 Maha seasons are well-reflected in this monthly RAI Drought Index. This index’s speciality is that it accurately depicts the occurrence of heavy rains in addition to drought, with good examples being identified as the 2010 Yala and 2015 Maha seasons.

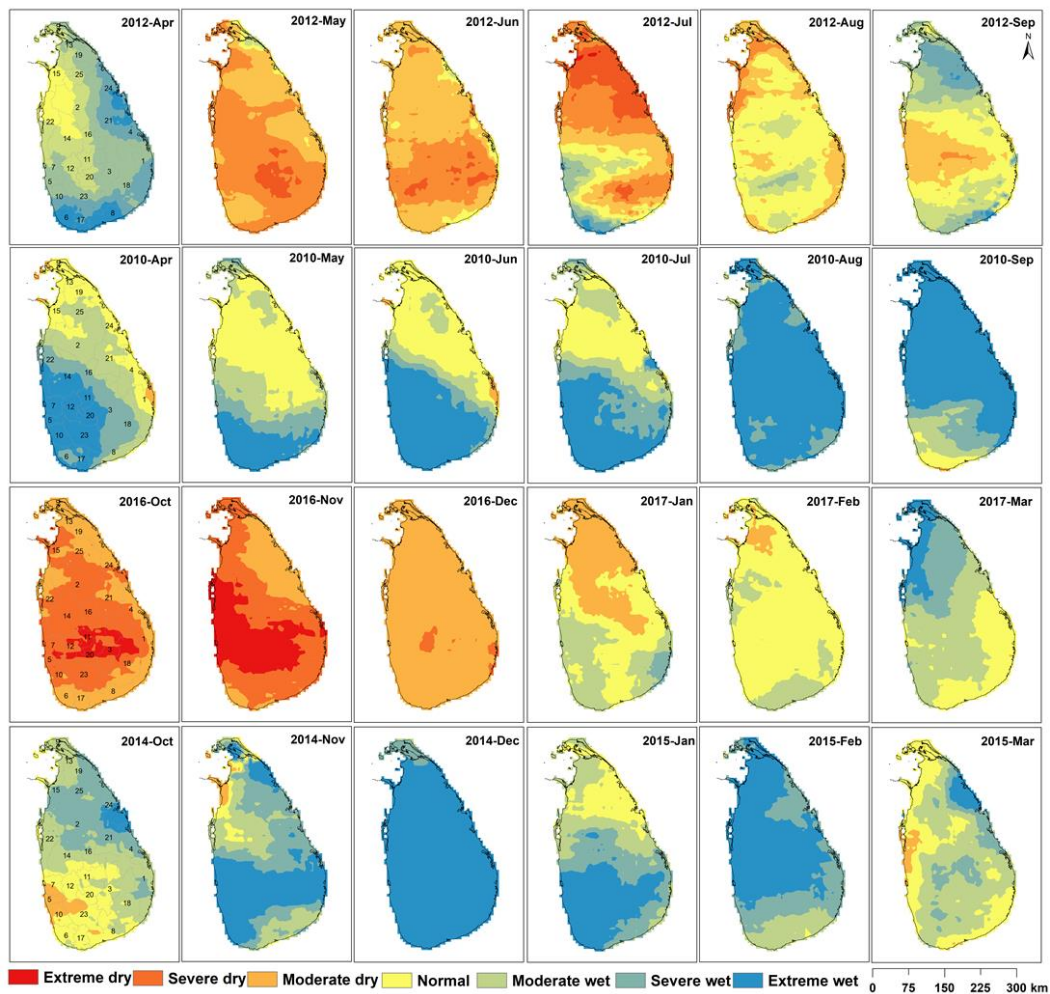


Figure 7. Monthly variation of Rainfall Anomaly Index (RAI) values over drought and non-drought years in Yala (2010, Non-drought Year; 2012, Drought Year) and Maha season (2014–2015, Non-drought year; 2016–2017, Drought year).

3.4. Standardized Precipitation Index (SPI)

Standardized Precipitation Index (SPI) is one of the most important indicators used consistently by various researchers and decision-makers to determine and monitor drought intensity. Furthermore, previously reported studies [72–75] have shown that the historical spatial-temporal distribution of meteorological droughts can be determined using this SPI index. In this study, CHIRPS rainfall data were used to calculate the SPI index from 1989 to 2019, covering each district using a World Meteorological Organization (WMO) tool at different time frames. SPI values can be well used to determine short-term and long-term drought.

SPI is a drought index widely used by decision-makers worldwide to identify, monitor, and determine droughts' severity. In this study, the SPI values at the district level in Sri Lanka were calculated for 3, 6, 9, 12, and 24 months from 1989 to 2019, as this index is designed to determine the meteorological drought for such different time scales. Soil moisture and crop health generally respond to short-term and small-scale rainfall changes, while long-term rainfall changes are reflected by changes in groundwater runoff and reservoir storage.

A 3-month SPI can be used to reflect short- and medium-term soil moisture changes and their seasonal reflections. Table 3 shows the change in SPI (3-month) values for drought (2016–2017) and non-drought years (2014–2015) during the Maha cropping season for all the 25 districts in Sri Lanka. The analysis of rainfall anomaly for the Maha season showed

that those two years were more suitable for understanding the SPI values changes during drought and non-drought periods. Here, it is clear that the SPI value is low during the drought season. In the Yala season, the early grain filling stage of paddy is in June, when the plants need to receive water. The decrease in soil moisture due to the rainfall decrease severely affects the crop yield. Moreover, October and November are the seasons when the Maha season begins with the cultivation of crops, and the occurrence of drought during this period leads to an increase in non-crop areas. As shown clearly with 3-month SPI values in Table 3, there was a severe drought in Sri Lanka during the 2016–2017 Maha season [76]. This had a significant impact on the paddy harvest in 2016 Maha, and 19 out of 25 districts in Sri Lanka were affected by the drought.

Table 3. Three-month SPI values for a good year (2014–2015) and a drought year (2016–2017).

District	2014–2015 Maha						2016–2017 Maha					
	Sep	Oct	Nov	Dec	Jan	Feb	Sep	Oct	Nov	Dec	Jan	Feb
Ampara	0.48	1.45	1.27	0.73	2.07	3.14	−1.61	−3.1	−1.29	−1.9	−1.09	−1.01
Anuradhapura	0.05	0.77	1.47	0.97	2.47	2.86	−1.95	−3.28	−2.3	−2	−0.82	−0.44
Badulla	0.29	0.92	1.01	0.73	0.76	1.84	−2.26	−3.46	−2.29	−2.19	−0.8	−0.72
Batticaloa	0.5	1.54	1.48	0.95	2.69	3.81	−1.24	−2.57	−1.32	−1.78	−1.1	−0.96
Colombo	0.82	0.93	1.16	0.61	1.68	1.77	−2.69	−3.29	−2.53	−1.93	−0.36	−0.66
Galle	0.51	1.65	1.67	0.84	1.51	1.75	−1.84	−2.24	−1.72	−1.25	−0.15	−0.32
Gampaha	0.76	0.84	1.18	0.91	1.94	2.14	−2.75	−3.71	−2.58	−2.14	−0.42	−0.86
Hambantota	0.19	1.55	1.12	0.46	0.85	1.48	−1.67	−2.35	−1.36	−1.49	−0.73	−0.74
Jaffna	0.52	0.31	1.42	1.34	0.71	2.5	−1.31	−3.01	−2	−1.89	−0.74	−0.2
Kalutara	0.75	1.23	1.43	0.72	1.5	1.6	−2.48	−2.82	−2.23	−1.7	−0.46	−0.6
Kandy	0.62	0.81	1.08	0.85	1.09	1.72	−2.42	−3.58	−2.23	−2.18	−0.71	−0.85
Kegalle	0.88	0.84	1.17	0.99	1.53	1.77	−2.81	−3.66	−2.53	−2.14	−0.4	−0.85
Kilinochchi	0.35	0.53	1.55	1.31	1.08	2.43	−1.51	−2.63	−1.92	−1.87	−0.8	−0.29
Kurunegala	0.55	0.81	1.35	1.19	2.07	2.69	−2.42	−3.71	−2.34	−2.12	−0.52	−0.55
Mannar	0.27	0.73	1.54	0.98	1.37	2.69	−2.2	−3.14	−2.51	−1.88	−0.7	−0.23
Matala	0.24	0.96	1.26	0.9	2.24	2.86	−2.13	−3.36	−2.18	−2.15	−0.89	−0.69
Matara	0.49	1.69	1.61	0.64	1.41	1.63	−1.86	−2.41	−1.82	−1.51	−0.49	−0.53
Moneragala	0.08	1.23	1.01	0.67	0.89	1.96	−1.91	−3.12	−1.41	−1.72	−0.72	−0.78
Mullaitivu	0.27	0.82	1.66	1.26	1.27	2.91	−1.48	−2.5	−2.03	−1.86	−0.95	−0.39
Nuwara Eliya	0.66	0.81	1.04	0.79	0.57	1.07	−2.67	−3.59	−2.64	−2.3	−0.73	−0.83
Polonnaruwa	0.22	1.23	1.56	1.09	3.53	3.53	−1.62	−2.86	−1.89	−1.84	−0.92	−0.71
Puttalam	0.47	0.81	1.57	1.32	1.92	2.78	−2.41	−3.89	−2.52	−2.1	−0.43	−0.38
Ratnapura	0.66	1.25	1.4	0.88	1.34	1.64	−2.29	−3.07	−2.31	−1.89	−0.52	−0.65
Trincomalee	0.34	0.94	1.48	1.18	3.31	3.34	−1.27	−2.45	−1.63	−1.5	−0.72	−0.4
Vavuniya	0.12	0.7	1.64	1.21	2.18	2.89	−1.77	−2.82	−2.08	−1.82	−0.84	−0.36

Figure 8 shows the 3, 6, 9, 12, and 24-month SPI values for the wet, intermediate, dry, and semiarid zones of Sri Lanka from 1989 to 2019, respectively. An important point to note from all the SPI analyses described above is that droughts' intensity in the dry zone is much higher than in the wet zone. This reflects well for the chronological variability of short- and long-term droughts. During the last 31 (1989 to 2019) years, which is the study period of this research, drought has been reported from various parts of Sri Lanka in the years 1989, 1992, 1996, 2000, 2001, 2002, 2004, 2009, 2012, 2013, 2014, 2016, 2017, and 2018, respectively as reported in various studies [12,14,77]. The SPI depicted in Figure 8 has captured well all the droughts mentioned above in most of the studied SPI time intervals.

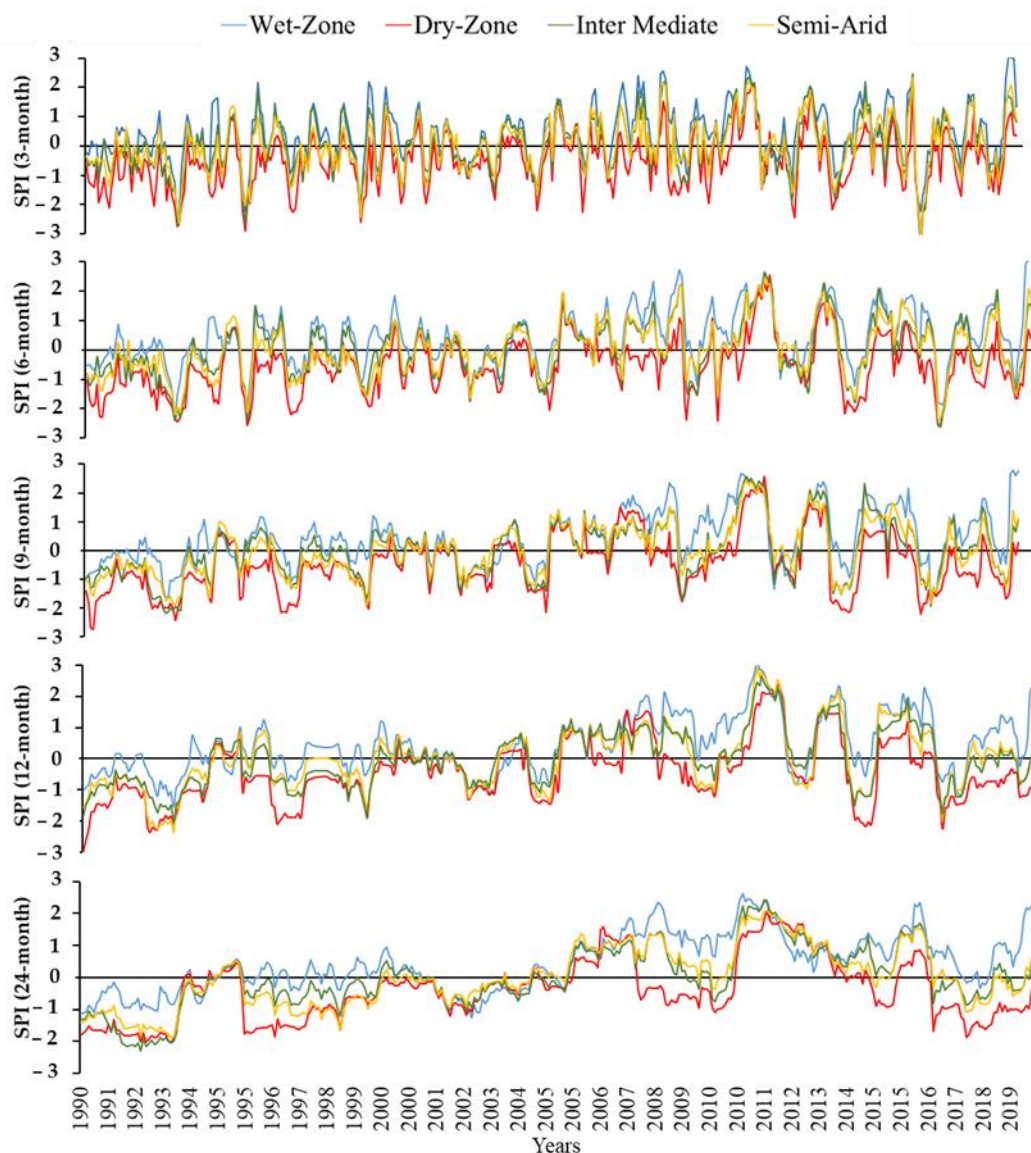


Figure 8. Shows how 3-month, 6-month, 9-month, 12-month, and 24-month SPI values vary from 1989 to 2019 for the wet, dry, intermediate, and semiarid climatic zones.

Although short-term drought is represented by 3-month SPI, long-term (6, 9, 12, or 24 months) SPI can be effectively used to determine the long-term drought behavior. The 6-month SPI has good potential to reflect the seasonal and medium-term rainfall trends, and changes in rainfall can also be detected for different periods. Confirming this, the SPI variation at 6, 9, 12, and 24 months accurately represented the long-term droughts of 2009, 2013, 2014 and the drought that continued from 2016 to 2018 in Sri Lanka. It is typical for agricultural as well as hydrological droughts to take a season or more to develop. The 9-month, 12-month, and 24-month SPIs provide accurate indications of interseasonal rainfall patterns, highlighting the impact on water flows, groundwater levels, and reservoir levels.

A closer observation of SPI variables reveals that the dry zone's SPI values are always lower in each timeframe than the other three zones. The other identification is that the semiarid region's drought pattern is similar to the intermediate zone's drought. The important thing that emerged from the detailed analysis of those drought years was that these droughts occurred in different periods, i.e., short-term and long-term. The droughts that occurred mainly in the dry zone during 2008–2009, 2013–2014, and 2016–2018 are the best examples of recent long-term droughts. SPIs have captured droughts and high rainfall (flood) years such as 2010, 2011, 2013, and 2015. The years 2013 and 2014 are

meteorologically critical years, as those periods alternate between the two Yala and Maha seasons of drought and non-drought.

4. Discussion

As the study focused on the monitoring of meteorological and agricultural drought and hazard mapping, long-term (31-year) monthly, seasonal, and annual rainfall variability at the district and climate zone level were analyzed for an overview of drought-affected seasons and districts. It was well-identified that the dry and semiarid zones of Sri Lanka receive significantly less rainfall during the NEM season. It is also a reason for more droughts during that season. Analysis of the number of days with different rainfall classes in climatic zones revealed that the number of days during which Light and Moderate occur during a drought is 20–30% lower than normal. However, this implies that the reduction in the number of rainy days in the Light and Moderate classes contributes more to the occurrence of drought than other classes. In other words, the occurrence and propagation of drought depend on the number of wet and dry days during a particular monsoon season. The most important thing that emerges here is the tendency for an apparent decrease in the number of rain-free days for all climate zones from 1990 to 2019. This shows that the dry weather in Sri Lanka is gradually declining. However, the number of dry days during the dry season is reduced by 20–40 days, compared to the year's average dry day.

RAI is important when referring to meteorological drought indicators, because it can be easily used to monitor how the drought has historically changed with the annual and seasonal rainfall variation. Importantly, this study shows a direct link between the droughts found in this study and the reported droughts. Although the incidence of drought during the Yala season was high before 2010, it has decreased since 2010, but the incidence of drought during the Maha season has increased. To better understand, the spatial and temporal variations of meteorological drought at monthly or quarterly selected dry and wet years were compared. Subsequent results show that, in both Yala and Maha seasons, the crop is affected by drought in both the early and mature stages. The SPI index was used to monitor the historical drought further using the periods of 1, 3, 6, 9, 12, and 24 months, during which time the variability of the drought from 1989 to 2019 was indicated to reflect the short- and long-term occurrence of the drought. In this study, the short-term and long-term events of droughts identified by the SPI analysis show a close relationship with the reported drought events [12,14,77].

4.1. Agriculture Drought Monitoring

In order to determine the relationship between meteorology and agricultural drought, the NDVI, LST, VCI, TCI, and VHI indices were analyzed as described herein. Variations in VCI and TCI were studied, assuming that most vegetation was stressed during the drought years and average in other years. A continuous decrease in the values of VCI and TCI or the longevity of low values is suitable for demonstrating dryness or crop stress level in a country, region, province, district, or a pixel of a satellite image. Figure 9 shows the VCI and TCI indices' spatial and temporal variability during the Yala (April to September) seasons of the drought year of 2012 and non-drought year of 2013.

The exciting thing to see here is how well the two indicators have successfully monitored drought and non-drought seasons. Annual RAI (Figure 5) and the SPI (Figure 7) analyses of 3-month, 6-month, and 9-month periods show that 2012 was a meteorological drought year, and 2013 was non-drought. The study of VCI and TCI also reveals that they are similarly observed, which concludes that the meteorological drought also turned into an agricultural drought in 2012. Further analysis of both the VCI and TCI indicators shows that farmers and their farms in the dry zone were the most affected by the drought and suffered from severe drought from June to August in 2012.

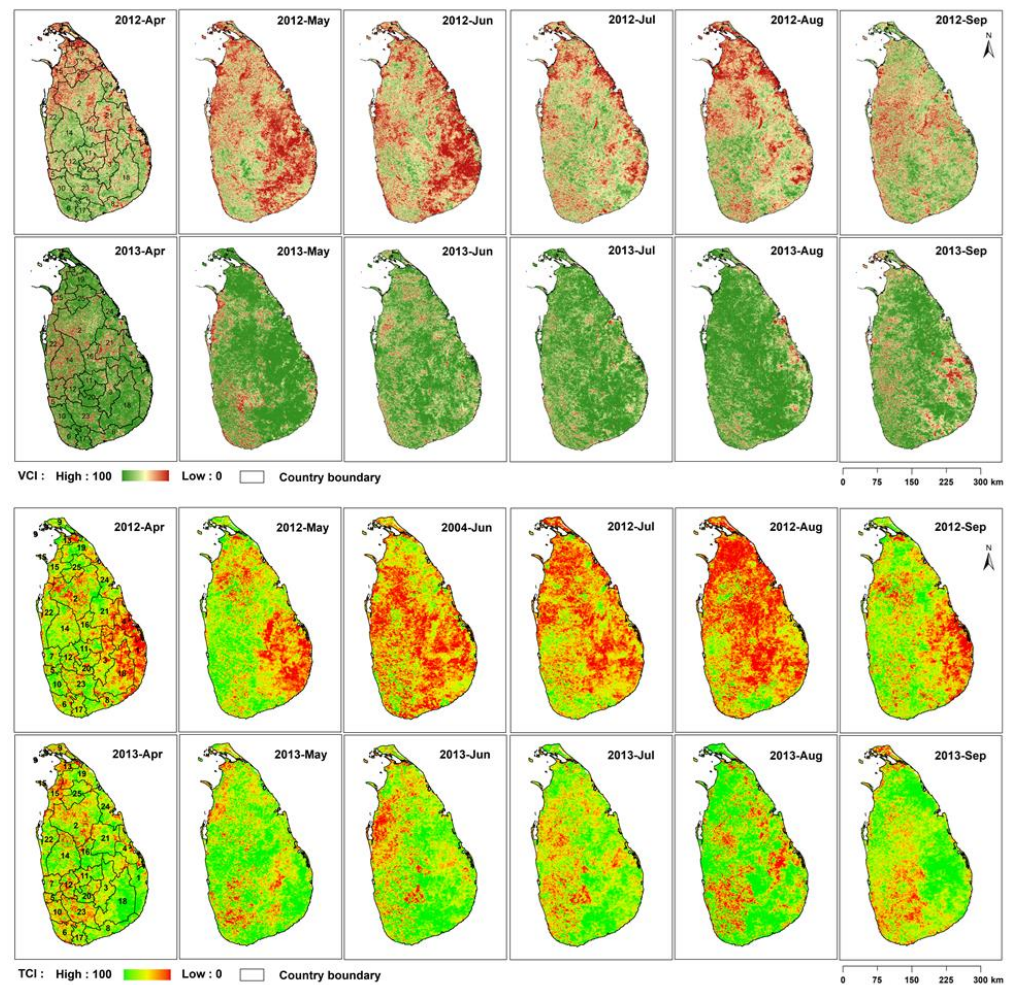


Figure 9. Vegetation Condition Index (VCI) and Temperature Condition Index (TCI) changes in drought and non-drought years.

Determining the intensity, spatial distribution, and duration of drought relative to a particular crop-season or year is essential in disaster management and decision-making. Similarly, if the spread and occurrence of drought can be calculated over several years in history, it is essential in drought management. Figure 10 shows the severity of the drought and spatial distribution from 2001 to 2019 using the VHI drought classification shown in Table 4. The maps thus generated a range from dark red to light yellow, with low VHI values representing extreme-to-moderate drought and green showing good, healthy crops. The significant drought years mapped via VHI for 2001 to 2019 are 2001, 2002, 2004, 2009, 2012, 2014, and 2016 and are very well coinciding with field information [11–15].

Table 4. Drought classification based on Vegetation Health Index (VHI) [78].

Drought Category	VHI Value
Extreme drought	$VHI \leq 10$
Severe drought	$10 < VHI \leq 20$
Moderate drought	$20 < VHI \leq 30$
Mild drought	$30 < VHI \leq 40$
No drought	$40 < VHI$

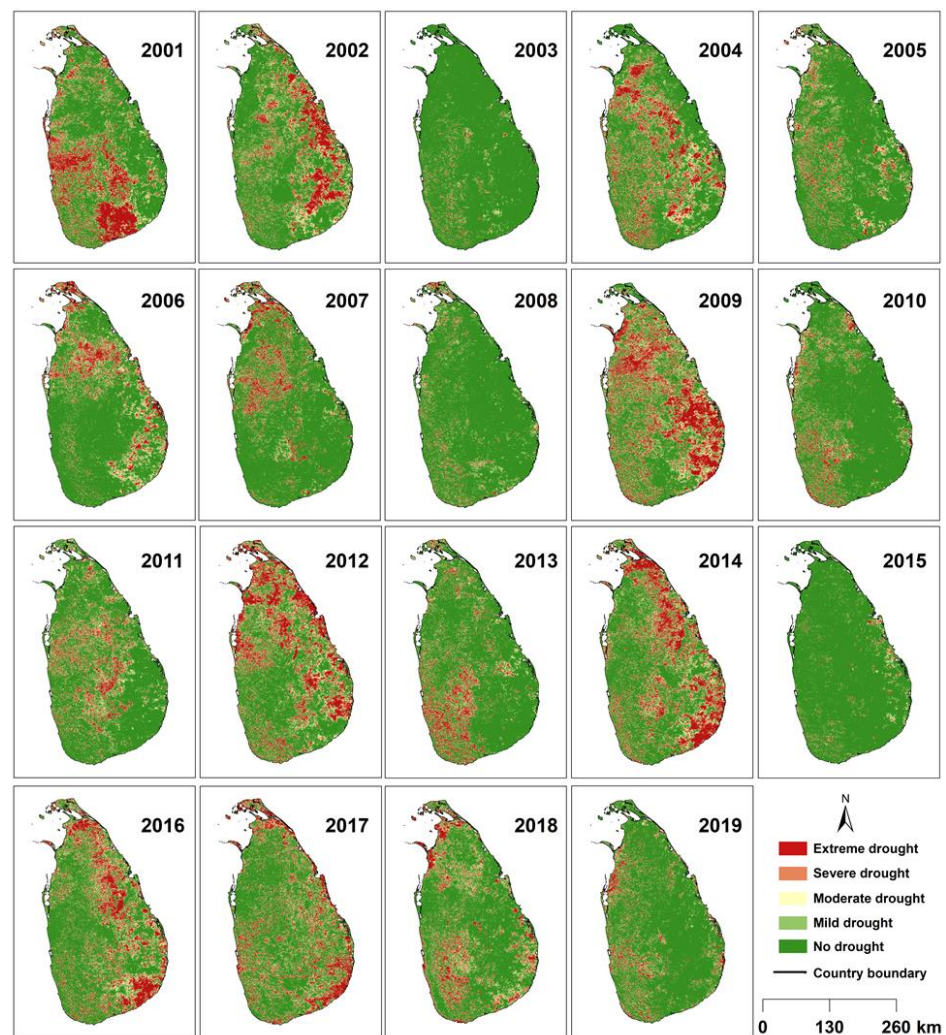


Figure 10. Spatial distribution of annual agriculture drought in Sri Lanka from 2001 to 2019.

4.2. Annual Drought Area, Its Classification, and Declaration

Variability of annual percentage of VHI drought classes' area of Sri Lanka is given by Table A3 in detail. Most importantly, that area percentage shows that the percentage of drought-prone areas of the Extreme category in Sri Lanka is more than 10% each year that droughts have reported. Furthermore, as the intensity of the drought increases, the extent of the extreme category's drought-prone areas to vary from 10% to 20%, with the 2001 and 2012 droughts showing the highest percentage of drought-prone areas in the extreme drought category. Overall, it is clear that the VHI index has captured the drought conditions in Sri Lanka in terms of both extreme and severe droughts.

The VHI's class area percentage-based methodology can be introduced as a quantitative approach to declare drought in Sri Lanka. This is done by combining the area percentages of the Extreme and Severe drought classes of VHI and classifying them into four drought area classes (DA classes), such as DA1, DA2, DA3, and DA4, as shown in Table 5.

As shown in Table 6, it is indicated that the drought can be declared if the DA classes become DA4. This is evidenced by the fact that Sri Lanka experienced severe droughts in 2001, 2009, 2012, and 2016 regarding population exposure and agriculture crop damage [12,14,75].

Table 5. Country-wide annual drought area percentage based on VHI drought classes.

Drought Area (DA) Classes	Area Percentage (A%)
DA1	$A\% < 10$
DA2	$10 \leq A\% < 20$
DA3	$20 \leq A\% < 30$
DA4	$A\% \geq 30$

Table 6. Country-wide annual drought area percentage for extreme (Ex) and severe (Se) drought classes, together with drought area (DA) classes, can be used for drought declaration.

Year	Ex–Se of VHI A%	DA Classes	Drought Declaration
2001	30.16	DA4	Yes
2002	20.91	DA3	-
2003	2.64	DA1	-
2004	20.00	DA2	-
2005	9.08	DA1	-
2006	14.90	DA2	-
2007	13.56	DA2	-
2008	4.62	DA1	-
2009	35.57	DA4	Yes
2010	9.62	DA1	-
2011	13.76	DA2	-
2012	30.42	DA4	Yes
2013	17.03	DA2	-
2014	29.15	DA3	-
2015	2.48	DA1	-
2016	30.15	DA4	Yes
2017	23.27	DA3	-
2018	16.72	DA2	-
2019	10.02	DA1	-

4.3. Drought Hazard Mapping

As shown in Figure 11, the districts were classified into different hazard classes, such as Low, Moderate, and High, using a natural-break classification scheme. Furthermore, RAI-based meteorological drought hazard maps shown in Figure 11b were generated by applying the same approach used in agriculture drought hazard mapping.

When observing both the meteorological and agricultural drought hazard maps, the districts where the majority of the geographical area falls in the wet zone do not show drought hazards, while the other three climate zones represent all the hazard classes. In particular, when only considering the district level meteorological drought hazard distribution, all districts that show a high percentage of the geographical area in dry and semiarid climate zones fall under medium to high hazard classes. Districts with a majority area of the intermediate zone represent low hazard, while districts in the wet zone do not show meteorological drought hazard.

A distinctive feature of the distribution of agricultural drought hazards at the district level is the high hazard of districts, where the majority of rain-fed crops are grown, and the moderate hazard of the districts in the dry zone, where most of the crops are irrigated. It is important to note that districts in the dry and semiarid zones have moderate-to-high drought hazards, when considering the distribution of these meteorological and agricultural drought hazards. In fact, discrepancies between meteorological and agricultural drought risk maps generated at the district level in Sri Lanka indicate that meteorological drought does not always translate into an agricultural drought and that the onset of agricultural drought depends on the nature of the crop being cultivated (rain-fed or irrigated). However, the main advantage of identifying the relevant drought hazard in districts or provinces is that, by establishing sustainable agriculture and economy in those districts, decision-makers can minimize the impact of drought on water and food shortages.

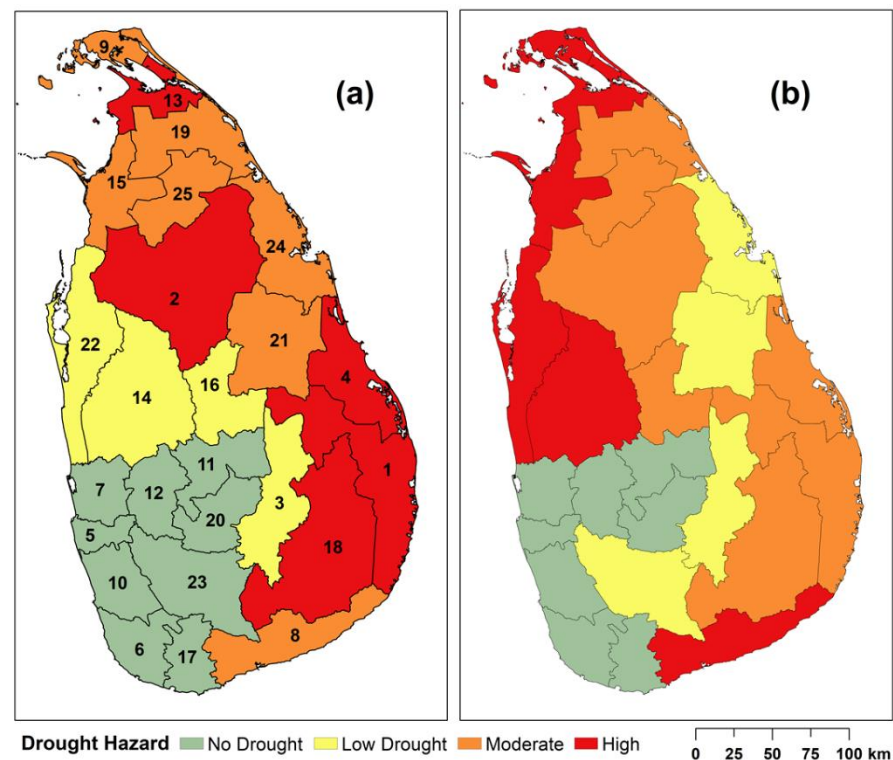


Figure 11. (a) Meteorological and (b) agricultural drought hazard at the district level in Sri Lanka.

In order to further understand the damage caused by drought on the country's economy, Figure 12 compares the years of severe drought in Sri Lanka from 1989 to 2019 and the percentage of gross domestic product (GDP) growth in the country. It can be clearly observed that the damage caused by the drought is directly related to the decline in the country's GDP. The main reason for this is the significant impact of drought on agriculture. A gradual decline in GDP between 2015 and 2019 is due to a combination of both drought and floods. However, this implies that proper drought hazard analysis can minimize the drought impact on agriculture and minimize damage to the country's economy. We strongly believe that monitoring drought will help policy makers and planners to capture the trend of drought and its distribution in Sri Lanka. Furthermore, the adopted methodology can be used in similar study areas in tropical regions to quantify the drought. At the same time, the present study will help to achieve sustainable development [79].

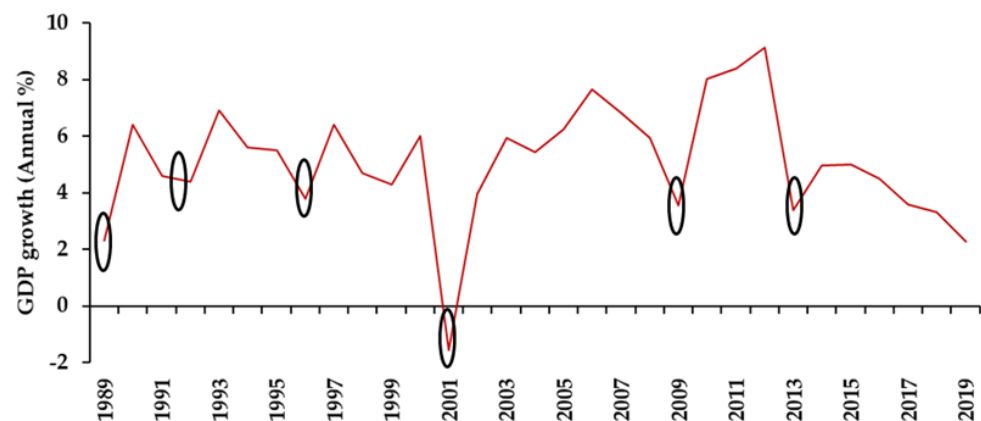


Figure 12. Annual % of gross domestic product (GDP) growth and drought occurrence; black circles represent the drought years [80].

5. Conclusions

In this study, SPI and RAI indicators, calculated with CHIRPS data, were used to monitor the meteorological drought in Sri Lanka from 1989 to 2019. Furthermore, VHI generated by MODIS-derived NDVI and LST was used from 2001 to 2019 to monitor agricultural drought. In addition, the SWM, NEM, FIM, and SIM monsoon seasons were studied in detail using five classes of rainfall, Light, Moderate, Rather Heavy, Heavy, and Very Heavy, as well as dry days, to understand the occurrence of drought in the wet, dry, intermediate and semiarid climates of Sri Lanka. The rainfall class study results revealed that the number of days of Light and Moderate occurring in all four climatic zones tends to increase. Therefore, all climatic zones appear to be moving in the direction of drought reduction, because the reduction in the number of days of Light, Moderate, and Heavy rainfall directly contributes to the drought. The variability of the dry days of the climatic zones suggests that the dry days for both Yala and Maha seasons show a significant decrease for all regions and that the increase in the number of dry days is directly related to the occurrence of drought. That is to say, the dryness in Sri Lanka has been surpassed, and the wetness has increased.

Using the CHIRPS data, the RAI, which is calculated annually, per monsoon, and monthly, can accurately monitor the occurrence of meteorological droughts and their temporal and spatial distributions. Another critical point that this RAI analysis suggests is that, although the Yala season was most prone to droughts before 2012, it has shifted since 2012 to the Maha season. The SPI, studied under different timeframes, provides excellent support for monitoring the variability of short-term and long-term droughts by district, province, and region.

VHI, a combination of VCI and TCI derived from MODIS NDVI and temperature data, was well-suited for monitoring and mapping the spatial and temporal distribution of agricultural drought in Sri Lanka. In both the Yala and Maha seasons, it was well-established that, when the VCI and TCI are less than 30%, the crop becomes stressed, and the gradual persistence or further decrease of VCI and TCI leads to agricultural drought. The meteorological drought results analyzed via SPI and RAI and the agricultural drought monitored via VHI are similar. Another important conclusion that can be drawn here is that meteorological drought does not always translate into an agricultural drought; for example, during the 2007–2008 and 2011–2012 Maha seasons, the meteorological drought showed some degree. However, it did not translate into an agricultural drought. The VHI index also confirms this. It can be confirmed that a quantitative approach can be given to the declaration of drought by using the area percentage of the Extreme and Severe classes, calculated using the VHI index. The most important finding of this study is that the country's GDP has declined sharply during the years of severe drought in Sri Lanka. It can be concluded that the drought has a direct impact on the country's economy.

This study demonstrates that the rainfall data provided by satellite estimates can be used for meteorological drought monitoring as a good substitute for data provided by sparsely distributed rainfall locations. Although the spatial resolution of these rainfall data is relatively low, the study further demonstrates the potential of remote sensing data and GIS technology in monitoring high-resolution agricultural droughts. This study's uniqueness is that it calculates the meteorological and agricultural drought hazard at the district level. This is because district-level hazard information provides an essential context in disaster management planning and decision-making. When considering agriculture, crop planning can be done effectively and sustainably for drought-prone areas so identified. This can be done by introducing drought-tolerant crops, changing crop patterns, making minor changes during the growing season, etc., so that sustainable agriculture can continue. Sri Lanka's forest cover has decreased significantly over the past few decades [81], which could have a significant impact on the increasing severity of droughts in Sri Lanka. Furthermore, a previous study [82] showed an increasing trend of annual rainfall in Sri Lanka. Therefore, deforestation and changes in rainfall patterns can be considered as a driving

force for drought, and there could be other factors, too. Thus, it is strongly recommended that future research should pay more attention to such studies.

Author Contributions: Conceptualization, N.A. and M.E.; Data curation, N.A.; Formal analysis N.A.; Investigation, N.A.; Methodology, N.A., M.E., and M.R.; Resources, N.A.; Validation, N.A., M.E. and M.R.; Visualization, N.A., M.E. and M.R.; Writing—original draft, N.A.; Writing—review and editing, N.A., M.E. and M.R. All authors have read and agreed to the published version of the manuscript.

Funding: This research received no external funding.

Institutional Review Board Statement: Not applicable.

Informed Consent Statement: Not applicable.

Data Availability Statement: Daily Gridded Rainfall data (CHIRPS data) is available at Climate Hazards Group InfraRed Precipitation corrected with stations data (https://data.chc.ucsb.edu/products/CHIRPS-2.0/global_daily/netcdf/p05/, accessed on 12 January 2021). MOA11A2 and MOD13A1 data downloaded from <https://search.earthdata.nasa.gov/search>, accessed on 12 January 2021.

Acknowledgments: The authors are thankful to the Climate Hazard Groups for providing the long-term observatory data (CHIRPS data) and the National Aeronautics and Space Administration relevant satellite data. Assistance and facilities provided by the International Water Management Institute (IWMI) and Department of Physics, University of Colombo, are highly acknowledged.

Conflicts of Interest: The authors declare no conflict of interest.

Appendix A

Table A1. Percentage of district area contribution to different climatic zones.

DISTRICT	District Area Percentage			
	Dry Zone	Wet Zone	Intermediate	Semiarid Zone
Ampara	83.32	0.00	11.12	5.56
Anuradhapura	80.27	0.00	0.00	19.73
Badulla	12.92	1.95	85.12	0.00
Batticaloa	100.00	0.00	0.00	0.00
Colombo	0.00	100.00	0.00	0.00
Galle	0.01	99.99	0.00	0.00
Gampaha	0.11	98.06	1.83	0.00
Hambantota	11.15	0.17	18.83	69.85
Jaffna	100.00	0.00	0.00	0.00
Kalutara	0.01	99.99	0.00	0.00
Kandy	0.00	46.54	53.46	0.00
Kegalle	0.00	100.00	0.00	0.00
Kilinochchi	100.00	0.00	0.00	0.00
Kurunegala	20.12	7.29	72.21	0.37
Mannar	39.36	0.00	0.00	60.64
Matale	33.73	0.62	65.65	0.00
Matara	0.00	85.09	14.91	0.00
Moneragala	53.61	0.00	36.82	9.57
Mullaittivu	100.00	0.00	0.00	0.00
Nuwara Eliya	0.00	70.06	29.94	0.00
Polonnaruwa	98.43	0.00	1.57	0.00
Puttalam	21.22	0.27	25.27	53.23
Ratnapura	11.81	70.11	17.65	0.43
Trincomalee	100.00	0.00	0.00	0.00
Vavuniya	97.35	0.00	0.00	2.65

Table A2. Mean monthly, seasonal, and annual rainfall for 25 districts in Sri Lanka from 1989 to 2019.

District	January	February	March	April	May	June	July	August	September	October	November	December	SWM	FIM	SIM	NEM	Annual
Ampara	237	145	75	100	77	30	43	67	68	191	327	339	57	87	259	241	1698
Anuradhapura	106	47	63	138	112	16	33	50	115	243	308	248	63	101	275	134	1480
Badulla	208	111	116	174	150	91	80	93	157	264	347	291	114	145	306	203	2082
Batticaloa	228	106	54	63	30	17	35	58	66	189	343	361	39	58	266	231	1550
Colombo	106	99	152	296	351	300	190	176	323	439	375	187	268	224	407	130	2994
Galle	141	114	162	252	420	272	182	183	332	380	359	200	278	207	370	152	2998
Gampaha	88	90	137	270	284	264	147	137	238	408	340	151	214	204	374	110	2554
Hambantota	138	79	78	120	125	66	43	62	68	166	267	182	73	99	217	133	1393
Jaffna	73	26	21	56	27	12	18	12	32	219	436	216	14	38	328	105	1147
Kalutara	137	120	173	309	434	320	207	202	390	427	397	224	311	241	412	160	3340
Kandy	178	110	127	218	167	181	140	140	199	330	337	262	166	173	334	183	2390
Kegalle	113	108	166	304	293	297	201	187	272	449	371	181	250	235	410	134	2942
Kilinochchi	85	33	29	78	19	13	14	19	41	191	396	232	13	54	294	117	1152
Kurunegala	82	64	107	210	166	110	68	67	116	322	293	157	105	159	307	101	1762
Mannar	77	41	56	118	60	13	10	18	125	209	341	202	43	87	275	107	1268
Matale	183	101	105	174	152	75	74	88	148	293	342	328	107	140	317	204	2064
Matara	146	115	152	198	329	240	138	155	253	317	345	201	223	175	331	154	2590
Moneragala	186	104	96	150	130	38	43	62	65	220	339	266	67	123	280	185	1698
Mullaitivu	107	39	39	98	47	12	19	33	81	204	421	266	37	68	313	137	1367
Nuwara Eliya	144	112	138	224	213	228	170	169	239	313	314	245	204	181	314	167	2509
Polonnaruwa	181	79	67	102	154	16	49	75	134	262	335	340	86	85	298	200	1795
Puttalam	64	41	78	174	120	46	26	37	106	257	271	139	67	126	264	81	1359
Ratnapura	145	127	177	261	317	254	160	164	249	339	361	206	229	219	350	159	2760
Trincomalee	164	61	36	61	78	18	53	63	97	200	373	317	60	49	287	181	1522
Vavuniya	110	43	48	118	90	14	42	46	114	212	387	260	59	83	299	138	1485
Wet Zone	127	111	159	268	332	278	179	176	285	385	356	197	1250	426	742	435	2877
Intermediate zone	160	99	114	190	164	109	81	88	140	289	330	247	583	304	619	506	1979
Dry zone	151	74	63	112	97	17	38	54	93	224	344	282	298	175	568	507	1521
Semiarid zone	103	55	70	136	84	18	16	36	84	200	281	183	239	206	482	342	1265

Table A3. Country-wide district's annual drought area percentage based on VHI drought classes.

Year	VHI Drought Classes (Area in Percentage)				
	Extreme	Severe	Moderate	Mild	No
2001	20.80	9.36	7.43	11.45	50.96
2002	13.62	7.29	10.07	12.10	56.92
2003	1.33	1.31	2.37	4.18	90.82
2004	11.35	8.65	11.17	13.14	55.69
2005	4.94	4.13	6.54	9.55	74.83
2006	8.66	6.24	8.49	10.59	66.02
2007	8.75	4.81	6.42	8.27	71.75
2008	2.40	2.22	3.96	6.84	84.59
2009	24.32	11.25	13.12	13.74	37.57
2010	5.67	3.94	5.57	7.57	77.25
2011	7.88	5.87	8.70	11.51	66.03
2012	20.78	9.64	11.33	12.60	45.64
2013	11.88	5.15	7.16	9.26	66.54
2014	19.93	9.22	11.19	12.04	47.62
2015	1.29	1.20	2.25	3.85	91.41
2016	19.42	10.73	10.86	12.74	46.25
2017	15.40	7.86	10.25	12.51	53.98
2018	10.00	6.72	9.18	11.58	62.53
2019	6.02	4.00	6.02	7.82	76.14

References

- Rossi, G. Drought mitigation measures: A comprehensive framework. In *Drought and Drought Mitigation in Europe*; Voght, J.V., Somma, F., Eds.; Kluwer: Dordrecht, The Netherlands, 2000.
- Payus, C.; Ann, H.L.; Adnan, F.; Besse Rimba, A.; Mohan, G.; Kumar Chapagain, S.; Roder, G.; Gasparatos, A.; Fukushi, K. Impact of Extreme Drought Climate on Water Security in North Borneo: Case Study of Sabah. *Water* **2020**, *12*, 1135. [[CrossRef](#)]
- Maybank, J.; Bonsai, B.; Jones, K.; Lawford, R.; O'Brien, E.G.; Ripley, E.A.; Wheaton, E. Drought as a natural disaster. *Atmos. Ocean*. **1995**, *33*, 195–222. [[CrossRef](#)]
- Mishra, A.K.; Desai, V.R. Drought forecasting using stochastic models. *Stochast. Environ. Res. Risk Assess.* **2005**, *19*, 326–339. [[CrossRef](#)]
- Centre for Research on the Epidemiology of Disasters (CRED); United Nations for Disaster Risk Reduction (UNISDR). *The Human Cost of Weather Related Disasters 1995–2015*; Centre for Research on the Epidemiology of Disasters and United Nations for Disaster Risk Reduction: Geneva, Switzerland, 2015; p. 30.
- Dai, A. Increasing drought under global warming in observations and models. *Nat. Clim. Chang.* **2012**, *3*, 52–58. [[CrossRef](#)]
- Cayan, D.R.; Das, T.; Pierce, D.W.; Barnett, T.P.; Tyree, M.; Gershunov, A. Future dryness in the southwest US and the hydrology of the early 21st century drought. *Proc. Natl. Acad. Sci. USA* **2010**, *107*, 21271–21276. [[CrossRef](#)]
- Leng, G.; Tang, Q.; Rayburg, S. Climate change impacts on meteorological agricultural and hydrological droughts in China. *Glob. Planet. Chang.* **2015**, *126*, 23–34. [[CrossRef](#)]
- Zhang, X.; Tang, Q.; Liu, X.; Leng, G.; Di, C. Nonlinearity of runoff response to global mean temperature change over major global river basins. *Geophys. Res. Lett.* **2018**, *45*, 6109–6116. [[CrossRef](#)]
- He, X.; Pan, M.; Wei, Z.; Wood, E.F.; Sheeld, J. A Global Drought and Flood Catalogue from 1950 to 2016. *Bull. Am. Meteorol. Soc.* **2020**, *101*, E508–E535. [[CrossRef](#)]
- Ministry of Disaster Management. *Sri Lanka National Report on Disaster Risk, Poverty and Human Development Relationship*; Ministry of Disaster Management: Vidya Mawatha, Colombo, Sri Lanka, 2009.
- Prasanna, R.P.I.R. Economic costs of drought and farmers' adaptation strategies; evidence from Sri Lanka. *J. Econ. Res.* **2018**, *5*, 61–79.
- Hazard Profile of Sri Lanka*; Disaster Management Centre, Ministry of Disaster Management: Vidya Mawatha, Colombo, Sri Lanka, 2012.
- Rajendram, K. An Assessment of Drought in Mannar District, Sri Lanka. *Int. J. Humanit. Appl. Soc. Sci.* **2019**, *4*, 11. [[CrossRef](#)]
- Sri Lanka Comprehensive Disaster Management Program*; Ministry of Disaster Management: Vidya Mawatha, Colombo, Sri Lanka, 2014. Available online: <http://www.disastermin.gov.lk/web/images/pdf/slcdmp%20english.pdf> (accessed on 12 January 2021).
- Wilhite, D. Drought preparedness in the U.S. In *Drought and Drought Mitigation in Europe*; Vogt, J.V., Somma, F., Eds.; Kluwer: Dordrecht, The Netherlands, 2000; pp. 119–132.
- Wilhite, D.A.; Glantz, M.H. Understanding the drought phenomenon: The role of definitions. *Water Int.* **1985**, *10*, 111–120. [[CrossRef](#)]

18. American Meteorological Society (AMS) Drought. 2013. Available online: <https://www2.ametsoc.org/ams/index.cfm/about-ams/ams-statements/statements-of-the-ams-in-force/drought/> (accessed on 15 December 2020).
19. Heim, R.R. A review of twentieth-century drought indices used in the united states. *Bull. Am. Meteorol. Soc.* **2002**, *83*, 1149–1165. [[CrossRef](#)]
20. Keyantash, J.; Dracup, J.A. An aggregate drought index: Assessing drought severity based on fluctuations in the hydrologic cycle and surface water storage. *Water Resour.* **2004**, *40*. [[CrossRef](#)]
21. Afzal, M.; Ragab, R. Drought Risk under Climate and Land Use Changes: Implication to Water Resource Availability at Catchment Scale. *Water* **2019**, *11*, 1790. [[CrossRef](#)]
22. Palmer, W.C. *Meteorological Drought. Research Paper No. 45*; U.S. Department of Commerce Weather Bureau: Washington, DC, USA, 1965. Available online: <https://www.ncdc.noaa.gov/temp-and-precip/drought/docs/palmer.pdf> (accessed on 20 December 2020).
23. Gibbs, W.J.; Maher, J.V. *Rainfall Deciles as Drought Indicators*; Bureau of Meteorology Bulletin No. 48; Commonwealth of Australia Meteorology: Canberra, Australia, 1967.
24. Shafer, B.A.; Dezman, L.E. Development of a Surface Water Supply Index (SWSI) to assess the severity of drought conditions in snowpack runoff areas. In Proceedings of the Western Snow Conference, Fort Collins, CO, USA, 19–23 April 1982; pp. 164–175.
25. Kogan, F.N. Remote sensing of weather impacts on vegetation in non-homogeneous areas. *Int. J. Remote Sens.* **1990**, *11*, 1405–1419. [[CrossRef](#)]
26. McKee, T.B.; Doesken, N.J.; Kleist, J. Drought monitoring with multiple time scales. In Proceedings of the 9th Conference on Applied Climatology, Dallas, TX, USA, 15–20 January 1995; pp. 233–236.
27. Keyantash, J.; Dracup, J.A. The quantification of drought: An evaluation of drought indices. *Bull. Am. Meteorol. Soc.* **2002**, *83*, 1167–1180. [[CrossRef](#)]
28. Ajaz, A.; Taghvaeian, S.; Khand, K.; Gowda, P.H.; Moorhead, J.E. Development and evaluation of an agricultural drought index by harnessing soil moisture and weather data. *Water* **2019**, *11*, 1375. [[CrossRef](#)]
29. Steinemann, A. Drought indicators and triggers: A stochastic approach to evaluation. *J. Am. Water Resour. Assoc.* **2003**, *39*, 1217–1233. [[CrossRef](#)]
30. Bhuiyan, C. Various Drought Indices for Monitoring Drought Condition in Aravalli Terrain of India. In Proceedings of the XXth ISPRS Conference, Istanbul, Turkey, 12–23 July 2004. Available online: <https://www.isprs.org/proceedings/XXXV/congress/comm7/papers/243.pdf> (accessed on 15 January 2021).
31. McKee, T.B.; Doesken, N.J.; Kleist, J. The relationship of drought frequency and duration to time scales. In Proceedings of the 8th Conference on Applied Climatology, Anaheim, CA, USA, 17–22 January 1993; pp. 179–184.
32. Guttman, N.B. Comparing the Palmer drought index and the standardized precipitation index. *J. Am. Water Res. Assoc.* **1998**, *34*, 113–121. [[CrossRef](#)]
33. Patel, N.R.; Chopra, P.; Dadhwal, V.K. Analyzing spatial patterns of meteorological drought using standardized precipitation index. *Meteorol. Appl.* **2007**, *14*, 329–336. [[CrossRef](#)]
34. Kumar, M.N.; Murthy, C.S.; Sessa Sai, M.V.R.; Roy, P.S. On the use of Standardized Precipitation Index (SPI) for drought intensity assessment. *Meteorol. Appl.* **2009**, *16*, 381–389. [[CrossRef](#)]
35. Kumar, M.N.; Murthy, C.S.; Sessa Sai, M.V.R.; Roy, P.S. Spatiotemporal analysis of meteorological drought variability in the Indian region using standardized precipitation index. *Meteorol. Appl.* **2012**, *19*, 256–264. [[CrossRef](#)]
36. Quiring, S.M.; Gansh, S. Evaluating the utility of the Vegetation Condition Index (VCI) for monitoring meteorological drought in Texas. *Agric. Meteorol.* **2010**, *150*, 330–339. [[CrossRef](#)]
37. Poonia, S.; Rao, A.S. Analysis of meteorological drought at arid Rajasthan using Standardized Precipitation Index. In Proceedings of the 92nd Meteorological Society Annual Meeting, New Orleans, Louisiana, 22–26 January 2012.
38. Dutta, D.; Kundu, A.; Patel, N.R. Predicting agricultural drought in eastern Rajasthan of India using NDVI and standardized precipitation index. *Geocarto. Int.* **2013**, *28*, 192–209. [[CrossRef](#)]
39. Zhang, A.; Jia, G. Monitoring meteorological drought in semiarid regions using multi-sensor microwave remote sensing data. *Remote Sens. Environ.* **2013**, *134*, 12–23. [[CrossRef](#)]
40. Belayneh, A.; Adamowski, J.; Khalil, B.; Ozga-Zielinski, B. Long-term SPI drought forecasting in the Awash River Basin in Ethiopia using wavelet neural network and wavelet support vector regression models. *J. Hydrol.* **2014**, *508*, 418–429. [[CrossRef](#)]
41. Juan, A.R.; Sofia, H.; Georgina, M. Using CHIRPS Dataset to Assess Wet and Dry Conditions along the Semiarid Central-Western Argentina. *Hindawi Adv. Meteorol.* **2019**, *18*. [[CrossRef](#)]
42. Hashim, M.; Reba, N.M.; Nadzri, M.I.; Pour, A.B.; Mahmud, M.R.; Mohd Yusoff, A.R.; Ali, M.I.; Jaw, S.W.; Hossain, M.S. Satellite-Based Run-Off Model for Monitoring Drought in Peninsular Malaysia. *Remote Sens.* **2016**, *8*, 633. [[CrossRef](#)]
43. Robock, A.; Vinnikov, K.Y.; Srinivasan, G.; Entin, J.K.; Hollinger, S.E.; Speranskaya, N.A.; Liu, S.; Namkhai, A. The Global Soil Moisture Data Bank. *Bull. Am. Meteorol. Soc.* **2000**, *81*, 1281–1299. [[CrossRef](#)]
44. Tang, Q.; Oki, T. Terrestrial water cycle and climate change: Natural and human-induced impacts. In *AGU Geophysical Monograph Series*; John Wiley: Hoboken, NJ, USA, 2016; p. 221.
45. Peng, J.; Loew, A.; Merlin, O.; Verhoest, N.E. A review of spatial downscaling of satellite remotely sensed soil moisture. *Rev. Geophys.* **2017**, *55*, 341–366. [[CrossRef](#)]

46. Tapley, B.D.; Bettadpur, S.; Ries, J.C.; Thompson, P.F.; Watkins, M.M. GRACE measurements of mass variability in the Earth system. *Science* **2004**, *305*, 503–505. [CrossRef]
47. Hao, Z.; Yuan, X.; Xia, Y.; Hao, F.; Singh, V.P. An overview of drought monitoring and prediction systems at regional and global scales. *Bull. Am. Meteorol. Soc.* **2017**, *98*, 1879–1896. [CrossRef]
48. Rivera, J.A.; Marianetti, G.; Hinrichs, S. Validation of CHIRPS precipitation dataset along the Central Andes of Argentina. *Atmos. Res.* **2018**, *213*, 437–449. [CrossRef]
49. Nabil, H.; Ali, M.; Driss, O.; Ahmed, B.; Moulay, D.H.; Hicham, S. CHIRPS precipitation open data for drought monitoring: Application to the Tensift basin, Morocco. *J. Appl. Remote Sens.* **2020**, *14*, 034526. [CrossRef]
50. Yoon, D.H.; Nam, W.H.; Lee, H.J.; Hong, E.M.; Feng, S.; Wardlow, B.D.; Tadesse, T.; Svoboda, M.D.; Hayes, M.J.; Kim, D.E. Agricultural Drought Assessment in East Asia Using Satellite-Based Indices. *Remote Sens.* **2020**, *12*, 444. [CrossRef]
51. Nicholson, S.E.; Farrar, T.J. The influence of soil type on the relationships between NDVI, rainfall, and soil moisture in semiarid Botswana. *Remote Sens. Environ.* **1994**, *50*, 107–120. [CrossRef]
52. Kogan, F.N. Application of vegetation index and brightness temperature for drought detection. *Adv. Space Res.* **1995**, *15*, 91–100. [CrossRef]
53. Seiler, R.A.; Kogan, F.; Wei, G. Monitoring weather impact and crop yield from NOAA AVHRR data in Argentina. *Adv. Space Res.* **2000**, *26*, 1177–1185. [CrossRef]
54. Wang, J.; Price, K.P.; Rich, P.M. Spatial patterns of NDVI in response to precipitation and temperature in the central Great Plains. *Int. J. Remote Sens.* **2001**, *22*, 3827–3844. [CrossRef]
55. Anyamba, A.; Tucker, C.J.; Eastman, J.R. NDVI anomaly patterns over Africa during the 1997/98 ENSO warm event. *Int. J. Remote Sens.* **2001**, *22*, 1847–1860.
56. Ji, L.; Peters, A.J. Assessing vegetation response to drought in the northern Great Plains using vegetation and drought indices. *Remote Sens. Environ.* **2003**, *87*, 85–98. [CrossRef]
57. Abeysingha, N.S.; Rajapaksha, U.R.L.N. SPI-Based Spatiotemporal Drought over Sri Lanka. *Hindawi Adv. Meteorol.* **2019**, *2020*, 10. [CrossRef]
58. Ekanayake, E.; Perera, K. Analysis of drought severity and duration using copulas in Anuradhapura, Sri Lanka. *Br. J. Environ. Clim. Chang.* **2014**, *4*, 312–327. [CrossRef]
59. Thushara, G.; George, M.H.; Jonathan, M.G. Spatiotemporal Patterns of Agricultural Drought in Sri Lanka: 1881–2010. *Int. J. Clim.* **2015**, *36*, 563–575. [CrossRef]
60. Arandara, K.P.; Attalage, R.A.; Jayasinghe, M.T.R. Thermal comfort with evaporative cooling for tropical climates. In Proceedings of the International Conference on Sustainable Built Environment, (ICSBE-2010), Kandy, Sri Lanka, 13–14 December 2010.
61. Nisansala, W.D.S.; Abeysingha, N.S.; Islam, A.; Bandara, A.M.K.R. Recent rainfall trend over Sri Lanka (1987–2017). *Int. J. Climatol.* **2020**, *40*, 3417–3435. [CrossRef]
62. Punyawardena, B.V.R. Identification of the potential of grooving seasons by the onset of Seasonal rains: A study in the region of the North central dry zone. *J. Natn. Sci. Found. Sri Lanka.* **2002**, *30*, 13–21. [CrossRef]
63. David, E.; Marie-Lena, H.; Maik, W. Who Suffers Most From Extreme Weather Events? Weather-Related Loss Events in 1998 to 2017. *Global Climate Risk Index*. 2019. Available online: www.germanwatch.org/en/cr (accessed on 6 January 2021).
64. Funk, C.; Peterson, P.; Landsfeld, M.; Pedreros, D.; Verdin, J.; Shukla, S.; Husak, G.; Rowland, J.; Harrison, L.; Hoell, A.; et al. The climate hazards infrared precipitation with stations—a new environmental record for monitoring extremes. *Sci. Data Nat.* **2015**, *2*, 150066. [CrossRef]
65. Wan, Z.; Li, Z.L. A physics-based algorithm for retrieving land-surface emissivity and temperature from EOS/MODIS data. *IEEE Trans. Geosci. Remote Sens.* **1997**, *35*, 980–996.
66. Anne, S.; Stefan, E.; Irmgard, N.; Jörg, M. Assessing vegetation variability and trends in north-eastern Brazil using AVHRR and MODIS NDVI time series. *Eur. J. Remote Sens.* **2013**, *46*, 40–59. [CrossRef]
67. Sandipan, M.; Srabanti, B.; Sandeep, S.; Kireet, K.; De Utpal, K. Investigation of dominant modes of monsoon ISO in the northwest and eastern Himalayan region. *Appl. Clim.* **2015**. [CrossRef]
68. Dutta, D.; Arnab, K.; Patel, N.R.; Saha, S.K.; Siddiqui, A.R. Assessment of agricultural drought in Rajasthan (India) using remote sensing derived Vegetation Condition Index (VCI) and Standardized Precipitation Index (SPI). *Egypt. J. Remote Sens. Space Sci.* **2015**, *18*, 53–63. [CrossRef]
69. Edwards, D.C.; McKee, T.B. *Characteristics of 20th Century Droughts in the United States at Multiple Time Scales*; Climatology Report, 97–2; Department of Atmospheric Sciences. Colorado State University: Fort Collins, Colorado, 1997; p. 155.
70. Kogan, F.; Salazar, L.; Roytman, L. Forecasting crop production using satellite-based vegetation health indices in Kansas, USA. *Int. J. Remote Sens.* **2012**, *33*, 2798–2814. [CrossRef]
71. Burt, T.P.; Weerasinghe, K.D.N. Rainfall Distributions in Sri Lanka in Time and Space: An Analysis Based on Daily Rainfall Data. *Climate* **2014**, *2*, 242–263. [CrossRef]
72. Almedej, j. Drought Analysis for Kuwait Using Standardized Precipitation Index. *Hindawi Publ. Corp. Sci. World J.* **2014**, *9*, 2014. [CrossRef]
73. Christos, A.K.; Stavros, A.; Demetrios, E.T.; George, A. Application of the Standardized Precipitation Index (SPI) in Greece. *Water* **2011**, *3*, 787–805. [CrossRef]

74. Guttman, N.B. Accepting the standardized precipitation index: A calculation algorithm. *J. Am. Water Resour. Assoc.* **1999**, *35*, 311–322. [[CrossRef](#)]
75. Pei, Z.; Fang, S.; Wang, L.; Yang, W. Comparative Analysis of Drought Indicated by the SPI and SPEI at Various Timescales in Inner Mongolia, China. *Water* **2020**, *12*, 1925. [[CrossRef](#)]
76. Disaster Management Centre. Situation Report—Sri Lanka 17th May 2018 at 1800 hrs. Ministry of Public Administration and Disaster Management: Colombo, Sri Lanka, 2017. Available online: https://reliefweb.int/sites/reliefweb.int/files/resources/Situation_Report__on_2018__1526529064.pdf (accessed on 10 January 2021).
77. Pani, P.; Alahacoon, N.; Amarnath, G.; Bharani, G.; Mondal, S.; Jeganathan, C. Comparison of SPI and IDSI applicability for agriculture drought monitoring in Sri Lanka. In Proceedings of the 37th Asian Conference on Remote Sensing, Colombo, Sri Lanka, 17–21 October 2016.
78. Cai, S.; Zuo, D.; Xu, Z.; Han, X.; Gao, X. Spatiotemporal variability and assessment of drought in the Wei River basin of China. Innovative water resource management. *Proc. IAHS* **2018**, *379*, 73–82. [[CrossRef](#)]
79. United Nations Transforming Our World. *The 2030 Agenda for Sustainable Development*; United Nations: New York, NY, USA, 2015; p. 16301.
80. World Bank Open Data, GDP Growth (Annual %)—Sri Lanka (1965–2019). Available online: <https://data.worldbank.org/indicator/NY.GDP.MKTP.KD.ZG?locations=LK> (accessed on 10 January 2021).
81. Ranagalage, M.; Gunarathna, M.H.J.P.; Surasinghe, T.D.; Dissanayake, D.; Simwanda, M.; Murayama, Y.; Morimoto, T.; Phiri, D.; Nyirenda, V.R.; Premakantha, K.T.; et al. Multi-Decadal Forest-Cover Dynamics in the Tropical Realm: Past Trends and Policy Insights for Forest Conservation in Dry Zone of Sri Lanka. *Forests* **2020**, *11*, 836. [[CrossRef](#)]
82. Alahacoon, N.; Edirisinghe, M. Spatial Variability of Rainfall Trends in Sri Lanka from 1989 to 2019 as an Indication of Climate Change. *Isprs Int. J. Geo-Inf.* **2021**, *10*, 84. [[CrossRef](#)]